

# Sorting of Membrane and Fluid at the Apical Pole of Polarized Madin-Darby Canine Kidney Cells

Som-Ming Leung, Wily G. Ruiz, and Gerard Apodaca\*

Renal-Electrolyte Division of the Department of Medicine, Laboratory of Epithelial Biology, and Department of Cell Biology and Physiology, University of Pittsburgh, Pittsburgh, Pennsylvania 15261

Submitted December 8, 1999; Revised February 18, 2000; Accepted March 21, 2000

Monitoring Editor: Suzanne R. Pfeffer

When fluid-phase markers are internalized from opposite poles of polarized Madin-Darby canine kidney cells, they accumulate in distinct apical and basolateral early endosomes before meeting in late endosomes. Recent evidence suggests that significant mixing of apically and basolaterally internalized membrane proteins occurs in specialized apical endosomal compartments, including the common recycling endosome and the apical recycling endosome (ARE). The relationship between these latter compartments and the fluid-labeled apical early endosome is unknown at present. We report that when the apical recycling marker, membrane-bound immunoglobulin A (a ligand for the polymeric immunoglobulin receptor), and fluid-phase dextran are cointernalized from the apical poles of Madin-Darby canine kidney cells, they enter a shared apical early endosome ( $\leq 2.5$  min at 37°C) and are then rapidly segregated from one another. The dextran remains in the large supranuclear EEA1-positive early endosomes while recycling polymeric immunoglobulin receptor-bound immunoglobulin A is delivered to a Rab11-positive subapical recycling compartment. This latter step requires an intact microtubule cytoskeleton. Receptor-bound transferrin, a marker of the basolateral recycling pathway, has limited access to the fluid-rich apical early endosome but is excluded from the subapical elements of the Rab11-positive recycling compartment. We propose that the term ARE be used to describe the subapical Rab11-positive compartment and that the ARE is distinct from both the transferrin-rich common recycling endosome and the fluid-rich apical early endosome.

## INTRODUCTION

Endocytosis is involved in multiple cellular functions, including recovery of exocytosed membrane, down-regulation of growth factor receptors, modulation of channel/receptor recycling in response to extracellular signals, degradation of internalized particles, antigen presentation, and maintenance of cell surface polarity (reviewed by Mukherjee *et al.*, 1997). Because inefficient sorting would disrupt normal cellular polarity and function, trafficking of proteins in the endocytic pathways is constantly modulated during development and in response to changes in the cell's extracellular milieu. Upon internalization, membrane and fluid are delivered to peripherally localized early endosomes. The small GTPase Rab5 and the Rab5 effector EEA1 are localized to these compartments (Gorvel *et al.*, 1991; Stenmark *et al.*, 1996). It is within the tubulovesicular elements of the early

endosome that fluid (as well as ligands dissociated from their receptors) is segregated from membranous cargo that will recycle back to the cell surface. Whereas dissociated ligands and fluid are delivered in a microtubule-dependent process to late endosomes and then lysosomes, recycling receptors and bulk membrane can be delivered to a pericentriolar recycling endosome (reviewed by Mukherjee *et al.*, 1997). The recycling endosome is composed of 50- to 60-nm tubular elements and is involved in the delivery of recycling receptors to the cell surface. Rab11 has been localized to the recycling endosome and *trans*-Golgi network of nonpolarized cells, and transport between recycling endosomes and the plasma membrane is thought to require the Rab11 GTPase (Ullrich *et al.*, 1996; Green *et al.*, 1997; Ren *et al.*, 1998).

Polarized epithelial cells have added complexity because they are capable of endocytosing macromolecules from either their apical or basolateral plasma membrane domain (Bomsel *et al.*, 1989). When fluid-phase markers are internalized for short periods of time from opposite poles of filter-grown Madin-Darby canine kidney (MDCK) cells, they label two spatially distinct populations of early endosomes: the peripheral basolateral early endosomes (BEE) that underlie the basolateral cell surface (up to the level of the tight

\* Corresponding author. E-mail address: gla6@pitt.edu.  
Abbreviations used: AEE, apical early endosome; ARE, apical recycling endosome; BEE, basolateral early endosome; CE, common recycling endosome; DAB, diaminobenzidine; IgA, immunoglobulin A; MDCK, Madin-Darby canine kidney; pIgR, polymeric immunoglobulin receptor; Tf, transferrin.

junctions), and the corresponding apical early endosomes (AEE) that lie between the apical plasma membrane and the Golgi complex (Bomsel *et al.*, 1989; Parton *et al.*, 1989). No mixing of fluid-phase markers is observed after incubation of  $\leq 10$  min at  $37^\circ\text{C}$ ; however, mixing of internalized fluid-phase markers is observed in a shared supranuclear late endosomal compartment after  $\geq 15$  min at  $37^\circ\text{C}$  (Bomsel *et al.*, 1989; Parton *et al.*, 1989). The meeting of these markers is prevented in cells treated with the microtubule-depolymerizing agent nocodazole.

Fluid-phase-labeled AEE and BEE of MDCK cells are biochemically distinct. AEE and BEE, labeled with fluid-phase markers for 10 min at  $37^\circ\text{C}$ , do not fuse in a cell-free assay that reconstitutes endosome-endosome fusion, whereas homotypic BEE-BEE and AEE-AEE fusion is observed in this system (Bomsel *et al.*, 1990). These observations led to the conclusion that no mixing of contents occurs between fluid-labeled AEE and BEE and that mixing occurs only in late endosomes. However, in both Caco-2 and MDCK cells, basolateral recycling transferrin (Tf) and its receptor have access to apical endosomal compartments that label with apically internalized membrane markers (Hughson and Hopkins, 1990; Knight *et al.*, 1995; Odorizzi *et al.*, 1996). In Caco-2 cells, this Tf-rich compartment is termed the common recycling endosome (CE) (Knight *et al.*, 1995). A similar compartment is thought to exist in MDCK cells (Odorizzi *et al.*, 1996). Moreover, the transcytotic movement of basolaterally internalized immunoglobulin A (IgA), a ligand for the polymeric immunoglobulin receptor (pIgR), requires sequential traffic between BEE and an apical endosomal compartment termed the apical recycling endosome (ARE) (Apodaca *et al.*, 1994; Barroso and Sztul, 1994).

Operationally, the ARE was originally defined as the endosomal compartment labeled with a 10-min pulse of an apically internalized membrane marker (Apodaca *et al.*, 1994). The ARE is composed of tubulovesicular elements that are found both above the nucleus in a supranuclear distribution and below the apical plasma membrane in a subapical distribution. The relationship between the supranuclear and subapical elements of the ARE is unclear. We suggested that the ARE, as originally defined, might represent several distinct compartments (Apodaca *et al.*, 1994). It is known that the subapical elements of the ARE receive membrane but little fluid. They are organized about the centrosome and are dispersed upon treatment with nocodazole, indicating that microtubules may be required for their organization. Tf is found in the supranuclear IgA-labeled elements of the ARE, but only limited colocalization of IgA and Tf is observed in the subapical elements of the ARE (Apodaca *et al.*, 1994). Although the exact relationship of the CE and the supranuclear and subapical elements of the ARE remains to be clarified, it is likely that the CE overlaps to some extent the supranuclear elements of the ARE.

A confluence of recent data suggests that sorting of basolaterally internalized cargo may occur in multiple compartments (Gibson *et al.*, 1998; Sheff *et al.*, 1999; Brown *et al.*, 2000). Initially, basolaterally internalized IgA, Tf, and fluid markers are delivered to BEEs (Apodaca *et al.*, 1994; Brown *et al.*, 2000). As these endosomes move toward the apical pole of the cell, the membrane markers are sorted away from fluid and the IgA and Tf are directed to the supranuclear CE, which also receives apically internalized membrane markers

(Brown *et al.*, 2000). Some Tf recycling may occur directly from the BEE (Sheff *et al.*, 1999). It is within the tubular evaginations of the CE that Tf is packaged in 60-nm vesicles and recycled back to the basolateral cell surface (Odorizzi *et al.*, 1996). The transcytosing IgA, sorted from Tf, is then delivered to the subapical elements of the ARE (Brown *et al.*, 2000). Exit of IgA from the subapical elements of the ARE may be via C-shaped vesicles (Gibson *et al.*, 1998). The similar pericentriolar, subapical distribution of Rab11 and Rab25 in MDCK cells suggests that these two GTPases may be markers of the subapical elements of the ARE (Casanova *et al.*, 1999). Similarly, Rab 17 has been shown to label a series of subapical tubules and to colocalize with transcytosing IgA. As such, it too may be a marker of the subapical elements of the ARE (Hunziker and Peters, 1998; Zacchi *et al.*, 1998).

Although these observations define the sites of sorting along the basolateral pathway, there is relatively little known about the sites of sorting at the apical pole of the MDCK cell. The goal of this analysis was to answer the following questions: Are membrane and fluid segregated at the apical poles of MDCK cells? If so, in which compartment does this sorting occur? Are there markers associated with these compartments? What is the role, if any, of microtubules in the sorting process? Finally, what is the relationship of the fluid-phase-labeled AEE and the supranuclear or subapical elements of the ARE or the Tf-rich CE?

## MATERIALS AND METHODS

### *Antibodies, Proteins, and Other Markers*

The following reagents were used: affinity-purified rabbit anti-Rab11 polyclonal antibodies (Zymed, South San Francisco, CA); purified mouse monoclonal anti-EEA1 antibody (Transduction Laboratories, San Diego, CA); rat anti-ZO1 hybridoma R40.76 (Dr. D.A. Goodenough, Harvard University, Cambridge, MA); affinity-purified rabbit polyclonal anti-human IgA antibodies (Jackson Immunoresearch Laboratories, West Grove, PA); affinity-purified rabbit or mouse polyclonal anti-canine Tf antibodies (Apodaca *et al.*, 1994); affinity-purified and minimal cross-reacting fluorescein, CY3, and CY5-conjugated secondary antibodies (Jackson Immunoresearch Laboratories); lysine-fixable 10,000-Da FITC- or Texas red-dextran (Molecular Probes, Eugene, OR); canine apo-Tf (Sigma Chemical, St. Louis, MO), which was loaded with iron as described previously (Apodaca *et al.*, 1994); and human polymeric IgA (Dr. J.P. Vaerman, Catholic University, Leuven, Belgium). IgA was conjugated to HRP with the use of an Actizyme peroxidase conjugation kit (Zymed) as detailed in the included protocol. Conjugates containing one or two HRP molecules were separated from overly conjugated IgA-HRP and free HRP by chromatography on an S-200 column (Pharmacia, Piscataway, NJ) with the use of PBS containing 0.01% (wt/vol) thimerosal as eluent. Biochemical assays confirmed that conjugated IgA-HRP was efficiently transcytosed.

### *Cell Culture*

MDCK strain II cells expressing the wild-type rabbit pIgR have been described (Breitfeld *et al.*, 1989a). Cells were maintained in MEM (Cellgro, Fisher Scientific, Pittsburgh, PA) supplemented with 10% FBS (Hyclone, Logan, UT), 100 U/ml penicillin, and 100  $\mu\text{g}/\text{ml}$  streptomycin in 5%  $\text{CO}_2/95\%$  air. To maintain a high level of receptor expression, new cells were thawed every 2 wk and were split 1:10 and passaged once weekly. For experiments, cells were cultured on 12-mm or 75-mm (diameter), 0.4- $\mu\text{m}$  (pore size) Transwells (Costar, Cambridge, MA) as described (Breitfeld *et al.*, 1989a).

Cells were fed each day after the second day of plating and used 3–4 d after culture.

### Internalization of Ligands and Fluid-Phase Markers, Stripping of Cell-Surface Ligands, and Nocodazole Treatment

Ligands and fluid-phase markers were internalized from the apical or basolateral surface of filter-grown MDCK cells. Before Tf internalization, the cells were incubated for 1 h at 37°C in MEM/BSA (MEM, HBSS, 0.6% [wt/vol] BSA, 20 mM HEPES, pH 7.4) to deplete intracellular stores of Tf and to allow for cell surface and filter-bound Tf to dissociate. All incubations in MEM/BSA were performed in a circulating water bath. For basolateral uptake of Tf, the cells were rinsed with MEM/BSA at 37°C and the bottom edge of the filter was carefully blotted to remove excess medium. The 12-mm Transwell unit was placed on a 50- $\mu$ l drop of MEM/BSA containing the ligand. For apical uptake, the cells were rinsed with MEM/BSA at the appropriate temperature, excess fluid was aspirated from the cell side of the 12-mm Transwell, and 150  $\mu$ l of ligand or fluid-phase marker, diluted in MEM/BSA, was added. All incubations were performed in a humid chamber. At the end of the experiment, cells were either rapidly chilled to 4°C or, if appropriate, fixed immediately.

In many of the experiments, cell-surface receptors and their ligands were stripped from the cell surface as follows. Cells were treated for 30 min at 4°C with 25  $\mu$ g/ml L-1-tosylamide-2-phenylethylchloromethyl-ketone-treated trypsin. Subsequently, the cells were washed twice with ice-cold MEM/BSA and once for 10 min with 125  $\mu$ g/ml soybean trypsin inhibitor dissolved in MEM/BSA. For morphological analysis, the cells were subsequently rinsed with PBS containing 0.5 mM MgCl<sub>2</sub> and 0.9 mM CaCl<sub>2</sub> (PBS<sup>+</sup>) and fixed immediately.

Nocodazole (Calbiochem, La Jolla, CA) was dissolved in DMSO at 33 mM and stored at -20°C. In all experiments in which this drug was used, cells were pretreated for 60 min at 4°C in the presence of 33  $\mu$ M nocodazole. The drug was included in subsequent incubations.

### Immunofluorescent Labeling and Scanning-Laser Confocal Microscopy

Cells were fixed with the use of either a pH-shift protocol (Apodaca *et al.*, 1994) or periodate-lysine-paraformaldehyde (Brown and Farquhar, 1989) and then processed as described previously (Apodaca *et al.*, 1994). Imaging was performed on a TCS confocal microscope equipped with krypton, argon, and helium-neon lasers (Leica, Deerfield, IL). Images were acquired with the use of a 100 $\times$  plan-apochromat objective (numerical aperture 1.4) and the appropriate filter combination. Settings were as follows: photomultipliers set to 600–800 mV, 1.0- $\mu$ m pinhole, zoom = 2.0–3.5, Kalman filter ( $n = 4$ ). The images (1024  $\times$  1024 pixels) were saved in TIFF, and the contrast levels of the images were adjusted with Photoshop (Adobe, Mountain View, CA) on a Power PC G-3 Macintosh computer (Apple, Cupertino, CA). The contrast-corrected images were imported into Freehand 8.0 (Macromedia, San Francisco, CA) and printed from a Kodak (Rochester, NY) 8650PS dye sublimation printer.

### Homogenization of MDCK Cells and Sucrose Flotation Gradient

After internalization of marker, the cells (grown on 75-mm Transwells) were gently scraped in PBS and centrifuged for 5 min at 400  $\times$  g, and the pellet was resuspended in HB (250 mM sucrose, 10 mM HEPES, pH 7.4, 0.5 mM EDTA, containing proteinase inhibitors), recentrifuged, and then homogenized by three to five passages through a 22-gauge needle, as described previously (Bomsel *et al.*, 1990). The resulting homogenate was centrifuged at 1000  $\times$  g for 15

min at 4°C to generate a postnuclear supernatant. Under these gentle conditions of homogenization, >95% of the fluid-phase marker (HRP) was retained in membrane-bound “vesicles,” which were pelleted when centrifuged at 100,000  $\times$  g. The postnuclear supernatant was brought to 40.2% (wt/wt) sucrose in a 1-ml volume and loaded into 12-ml polycarbonate tubes and then overlaid successively with 3 ml of 35% (wt/wt) sucrose, 3 ml of 25% (wt/wt) sucrose, and 3 ml of 8.5% (wt/wt) sucrose (the sucrose solutions contained 0.5 mM EDTA and 10 mM HEPES, pH 7.4, as buffer). The gradients were then centrifuged for 60 min at 4°C in a TH641 swinging-bucket rotor (Sorvall, Wilmington, DE) at 35,000 rpm. Fractions (450  $\mu$ l) were collected from the top of the gradient. HRP activity was measured with the use of 0.1 mg/ml tetramethylbenzidine dihydrochloride substrate (Sigma, catalogue number T-3405) dissolved in phosphate-citrate-perchlorate buffer (Sigma, catalogue number P4922). The reaction was stopped by the addition of one-fifth volume of 2 M H<sub>2</sub>SO<sub>4</sub>, the time was noted, and the A<sub>450</sub> was recorded. One unit of HRP activity increased the A<sub>450</sub> by 0.01 absorbance units/min. Protein was measured with the use of the Pierce (Rockford, IL) bicinchoninic acid kit with BSA as a standard.

### Diaminobenzidine Density-Shift Assay

We have used a modified version of the diaminobenzidine (DAB) density-shift assay described previously (Apodaca *et al.*, 1994). [<sup>125</sup>I]IgA (5  $\mu$ g/ml) and 5–10 mg/ml HRP (Pierce) were cointernalized from the apical pole of the cells. In some experiments, cells were treated with nocodazole as described above. The concentration of HRP was adjusted so that equivalent amounts of HRP were retained by the cell at the end of the 2.5-min pulse or a 2.5-min pulse followed by a 7.5-min chase. After internalization, the cells were washed with ice-cold MEM/BSA. [<sup>125</sup>I]IgA was stripped from the apical cell surface with 100  $\mu$ g/ml tosyl-phenylmethyl-chloromethyl ketone-treated trypsin (Worthington, Freehold, NJ) (in MEM/BSA) three times for 10 min at 4°C. Alternatively, [<sup>125</sup>I]Tf was internalized from the basolateral cell surface for 30 min at 37°C, and HRP (5–10 mg/ml) was cointernalized from the apical pole of the cell during the last 7.5 min of the Tf pulse. These Tf-loaded cells were rapidly chilled and washed three times for 10 min. To allow for internalization of cell surface-bound Tf, the cells were warmed to 37°C for 2.5 min. HRP was included in the apical medium during this 2.5-min chase.

After ligand internalization and cell surface stripping, cells were washed twice with ice-cold HBSS containing 0.9 mM CaCl<sub>2</sub>, 0.5 mM MgCl<sub>2</sub>, and 20 mM HEPES, pH 7.4 (HBSS<sup>+</sup>). DAB reaction buffer (0.5 ml) was added to both apical and basal compartments of the Transwell. DAB reaction buffer was prepared by adding 3.3 ml of 3 mg/ml DAB (dissolved in HBSS<sup>+</sup>, pH adjusted to 7.4 with NaOH, and filtered) and 20  $\mu$ l of 30% (vol/vol) H<sub>2</sub>O<sub>2</sub> to 20 ml of HBSS<sup>+</sup>. In control reactions, H<sub>2</sub>O<sub>2</sub> was omitted from the DAB reaction buffer. After a 45-min incubation at 4°C, the cells were washed two times with HBSS<sup>+</sup>, and the filters were carefully excised from their holders, boiled in 0.4 ml of SDS lysis buffer (0.5% [wt/vol] SDS, 100 mM triethanolamine, pH 8.6, 5 mM EDTA, 0.02% [wt/vol] Na<sub>2</sub>S<sub>2</sub>O<sub>8</sub>) for 90 s, and shaken for 15 min at 4°C. Under these conditions, <5% of the total counts were associated with the detergent-treated filter. The supernatants were then centrifuged at 100,000  $\times$  g in an RP70AT rotor (Sorvall) for 25 min at 20°C in an RCM100 centrifuge (Sorvall). Radioactivity was quantified with a gamma counter. Values were normalized to reactions in which [<sup>125</sup>I]IgA and IgA-HRP were cointernalized from the apical pole of the cell, as described previously (Apodaca *et al.*, 1994).

### Immunoperoxidase Electron Microscopy and Immunogold Labeling

After internalization of IgA-HRP from the apical pole of the cell, plasma membrane-bound ligand was stripped with trypsin and the cells were fixed with the use of a pH-shift protocol as described

above. The cells were rinsed three times with 200 mM Na cacodylate buffer, pH 7.4, and then incubated with 0.1% (wt/vol) DAB dissolved in 200 mM cacodylate buffer for 2 min at room temperature. The DAB solution was aspirated, replaced with fresh DAB solution containing 0.01% (vol/vol) H<sub>2</sub>O<sub>2</sub>, and incubated for 30 min at room temperature in the dark. Cells were then washed with ice-cold KTM buffer (115 mM potassium acetate, 2.5 mM magnesium acetate, 4 mM EGTA, 2 mM calcium carbonate, 20 mM HEPES, pH 7.4, 1 mM DTT), and the plasma membrane was permeabilized with 200 µg/ml digitonin (dissolved in KTM buffer) for 20 min at 4°C. The cells were washed three times for 5 min with KTM buffer. Unreacted fixative was quenched with 40 mM glycine dissolved in PBS, and nonspecific protein-binding sites were blocked with PBS containing 2% (wt/vol) BSA (PBS-BSA) for 15 min at room temperature. The cells were incubated with anti-Rab11 antibodies and diluted 1:100 in PBS-BSA for 60 min at room temperature. The cells were washed three times for 5 min each with PBS-BSA and then incubated with protein A–5 nm gold (purchased from Dr. Jan Slot, Utrecht University, Utrecht, the Netherlands; diluted in PBS-BSA) for 60 min at room temperature. After three 5-min washes with PBS-BSA, the cells were fixed with 2.0% (vol/vol) glutaraldehyde in 100 mM Na cacodylate, pH 7.4, containing 1 mM CaCl<sub>2</sub>, 0.5 mM MgCl<sub>2</sub> for 30 min at room temperature. Samples were rinsed with 100 mM Na cacodylate, pH 7.4, and osmicated with 1.5% OsO<sub>4</sub> (wt/vol), 100 mM Na cacodylate, pH 7.4, 1% (wt/vol) K<sub>4</sub>Fe(CN)<sub>6</sub> for 30 min at room temperature. After several rinses with H<sub>2</sub>O, the samples were stained en bloc overnight with 0.5% (wt/vol) uranyl acetate in H<sub>2</sub>O. Filters were dehydrated in a graded series of ethanol, embedded in the epoxy resin LX-112 (Ladd, Burlington, VT), and sectioned with a diamond knife (Diatome, Fort Washington, PA). Sections, green in color (~250 nm), were mounted on butvar-coated nickel grids and viewed at 100 kV in a JEOL (Tokyo, Japan) 100 CX electron microscope without further contrasting.

## RESULTS

### *Sorting of Apically Internalized Membrane and Fluid Markers Is Rapid at 37°C*

To characterize potential sites for sorting, we determined the kinetics of membrane and fluid segregation at the apical poles of MDCK cells. As a membrane marker, we used apically internalized IgA, a ligand for the pIgR. Although the pIgR is cleaved at the apical pole of the MDCK cell, a significant fraction of the receptor escapes cleavage and can be internalized from the apical cell surface (Breitfeld *et al.*, 1989b). pIgR–IgA complexes internalized from the apical pole of the cell are rapidly and efficiently recycled back to the apical pole of the cell (Breitfeld *et al.*, 1989b; Apodaca *et al.*, 1994) and as such are markers of the apical recycling pathway. Less than 3% of IgA internalized from the apical surface of the cell is transcytosed and released at the basolateral pole of the cell (Breitfeld *et al.*, 1989b; Apodaca *et al.*, 1994). As described previously, we used FITC-dextran as a marker of fluid-phase uptake (Apodaca *et al.*, 1994).

In our first set of experiments, we cointernalized IgA and FITC-dextran from the apical pole of the cell for a short pulse (2.5 min at 37°C) and determined if these markers colocalized or whether they were sorted from one another (Figure 1, A–F). Colocalization was assessed by simultaneously acquiring dual-color fluorescent images of fixed and stained cells with a scanning-laser confocal microscope and digitally merging the images. Regions of colocalization appear yellow in the micrographs. The cells were also stained with an antibody that recognizes the tight junction-associated protein ZO1, because this structure serves as a convenient land-

mark to identify the border between the apical and basolateral plasma membrane domains. In Figure 1, ZO1 appears as a thin red line that surrounds each cell. Shown are two optical sections (nominally 1.5 µm apart) taken from the apical pole of the cell (Figure 1, A–F). Sections directly above the nucleus and from the lateral or basal pole of the cell are not shown because the majority of labeled structures were within 2–3 µm of the apical plasma membrane. When FITC-dextran and IgA were cointernalized for 2.5 min at 37°C, a significant degree of colocalization of the two markers was observed in all focal planes. The labeled compartments had a vesicular appearance, were relatively large, and were concentrated in a supranuclear focal plane coincident with the brightest ZO1 staining (Figure 1, D–F). There were few labeled structures in the apical-most sections (i.e., those closest to the apical plasma membrane; Figure 1, A–C). Although some IgA-labeled structures were found above the nucleus, little of the FITC-dextran was found in this position. No staining of either marker was observed at the basal pole of the cell.

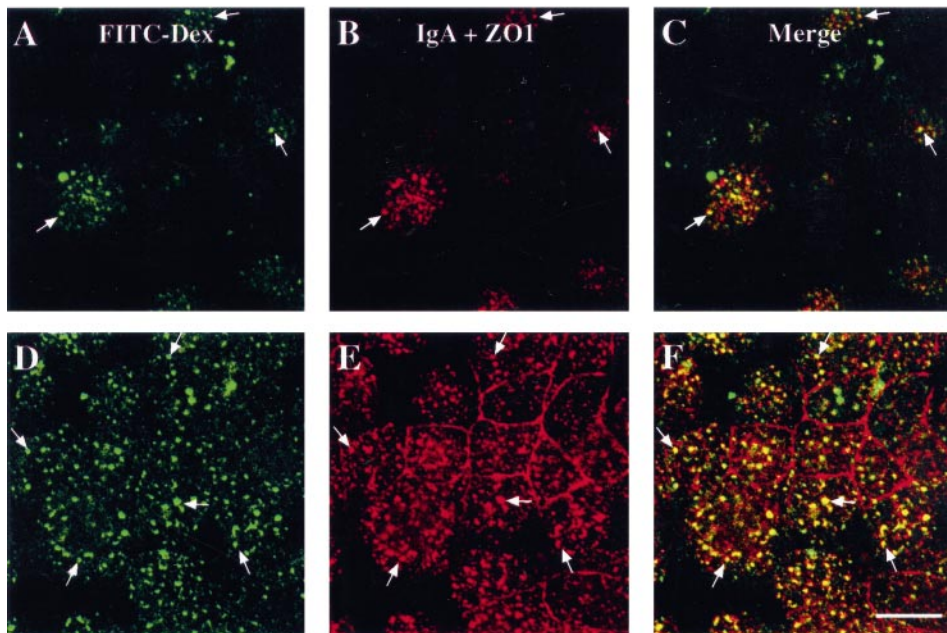
Sorting of the two markers became apparent when the 2.5-min pulse was followed by a 7.5-min chase in the absence of added marker. Although a fraction of the IgA remained colocalized with the FITC-dextran in the larger vesicular endosomes (Figure 1, I and L, arrows), a larger fraction of IgA was associated with numerous fine puncta that did not colocalize with the FITC-dextran (Figure 1, I and L). Some of the IgA-labeled endosomes were in close proximity to the nucleus. Unlike in the shorter internalization protocol, IgA internalized with the use of the pulse-chase protocol was localized to abundant small punctate structures that accumulated at the apical pole of the cell in a subapical distribution (Figure 1H). FITC-dextran-labeled structures were less concentrated in these apical sections (Figure 1G). Sorting of the IgA and FITC-dextran markers was also apparent when IgA and FITC-dextran were cointernalized for 5–10 min at 37°C. Again, IgA was found in small punctate structures that accumulated under the apical plasma membrane, most of which did not colocalize with FITC-dextran.

Whereas IgA moved from supranuclear endosomes to a subapical endosomal compartment, we observed little difference in the distribution of the fluid-phase marker after a 2.5-min pulse with or without a chase. In fact, if a 7.5-min pulse of Texas Red–dextran was followed by a 2.5-min pulse of FITC-dextran (in the continued presence of Texas Red–dextran), almost all of the labeled endosomal structures colocalized. These results confirm that the distribution of the fluid-phase marker remains largely unchanged after a 10-min internalization period.

### *Sorting of Membrane and Fluid Markers Is Observed in Flotation Gradients and in Density-Shift Assays*

To confirm that sorting had occurred under the conditions described above, we analyzed the distribution of [<sup>125</sup>I]IgA- and HRP-labeled endosomes in flotation gradients (Gruenberg *et al.*, 1989; Bomsel *et al.*, 1990). HRP is a classic marker of the fluid phase. [<sup>125</sup>I]IgA and HRP were cointernalized for 2.5 min at 37°C from the apical poles of the MDCK cells, and the cells were either rapidly chilled or incubated in marker-free medium for 7.5 min at 37°C. The cells were homogenized, and the postnuclear supernatant from a low-speed

## IgA + FITC-Dextran 2.5' Ap



## IgA + FITC-Dextran 2.5' Ap / 7.5' Chase

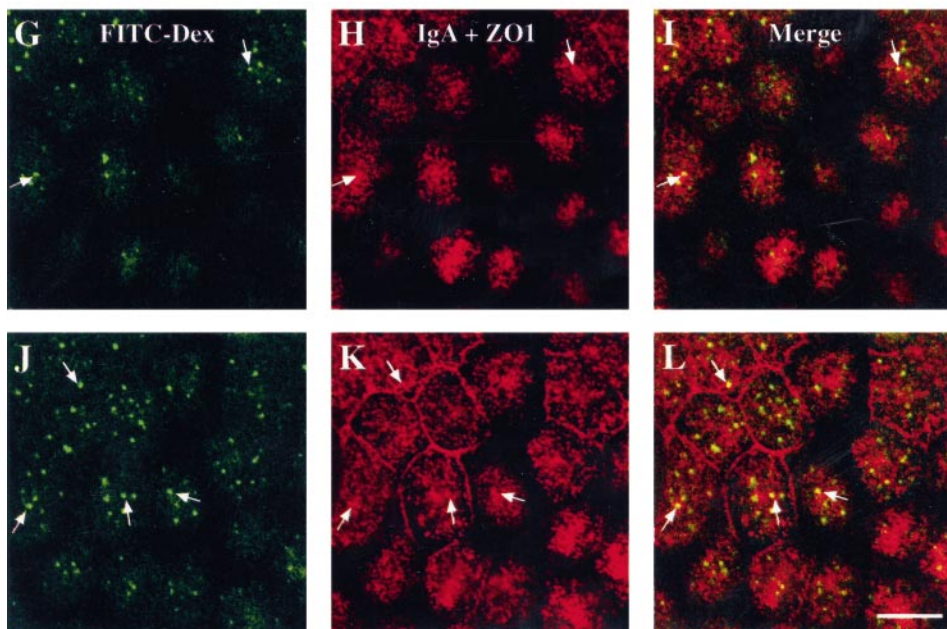


**Figure 1.** Distribution of IgA and FITC-dextran cointernalized from the apical pole of the cell for 2.5 min at 37°C (A–F) or with a 2.5-min pulse followed by a 7.5-min chase at 37°C (G–L). After IgA and FITC-dextran internalization, the cells were rapidly cooled, cell surface IgA was removed by trypsin treatment, and the cells were fixed with paraformaldehyde-lysine-periodate fixative. The fixed cells were incubated with IgA- and ZO1-specific primary antibodies and then reacted with CY5-labeled secondary antibodies. The CY5 signal is shown in the center panels, the FITC signal is shown in the left panels, and merged images of the CY5 and FITC signals are shown in the right panels. ZO1 appears as a thin red line at the periphery of each cell. Single optical sections, obtained with a confocal microscope, are shown from the apex of the cell (A–C and G–I) or at the level of the tight junctions (D–F and J–L). Note that the cells in the lower right corner of each panel, in panels G–L, are shorter than the cells in the upper left corner. Representative regions of colocalization are marked with arrows. Bars, 10  $\mu$ m.

centrifugation was adjusted to 40.2% sucrose and overlaid with 35, 25, and 8.5% (wt/wt) sucrose. The samples were centrifuged, and fractions were collected from each gradient. In these gradients, plasma membrane and Golgi are found at the interface between the 40.2 and 35% sucrose layers, whereas fluid-labeled early endosomes are found at the interface of the 35 and 25% sucrose layers. Late endosomes float to the interface between the 25 and 8.5% sucrose layers (Gruenberg *et al.*, 1989).

After the 2.5-min chase at 37°C, the majority of [<sup>125</sup>I]IgA and HRP activity was found at the 35/25% interface, as expected for proteins residing in early endosomes (Figure 2A). Although the HRP displayed a sharp peak, the [<sup>125</sup>I]IgA peak trailed toward the denser fractions, suggesting that some sorting may have already occurred under these conditions. When the 2.5-min pulse was followed by a 7.5-min chase, segregation of the [<sup>125</sup>I]IgA and HRP became more apparent (Figure 2B). Although the HRP remained in a sharp peak at the 35/25% interface, the peak of [<sup>125</sup>I]IgA activity shifted toward the denser fractions. These observations are consistent with the morphological analysis presented above and provide evidence that fluid-phase markers remained in the AEE while pIgR-bound IgA was sorted and delivered to a physically distinct compartment.

Sorting of fluid and membrane markers was also confirmed by use of a modified density-shift assay (Apodaca *et al.*, 1994). Based on the morphological data presented above, one would predict that under short internalization conditions there would be maximal colocalization of the IgA and HRP. If the IgA was sorted away from the fluid marker during a subsequent chase, less colocalization of the two markers would be expected. [<sup>125</sup>I]IgA and HRP were cointernalized for 2.5 min at 37°C and then either placed on ice or chased for an additional 7.5 min at 37°C. After the pulse-chase protocol, cell surface [<sup>125</sup>I]IgA was removed by trypsin treatment, and the cells were reacted with DAB reagent. In the presence of H<sub>2</sub>O<sub>2</sub>, the HRP catalyzes a reaction that cross-links the contents of the HRP-associated vesicles into a detergent-insoluble complex that can be recovered by centrifugation. After a 2.5-min pulse, ~95% of the [<sup>125</sup>I]IgA was found in HRP-labeled endosomes (Figure 2C). In contrast, after the 7.5-min chase, the amount of [<sup>125</sup>I]IgA found in the HRP-labeled endosomes had decreased by 50%. These results are consistent with the morphological evidence presented above that fluid and membrane are delivered to a common AEE and then rapidly sorted from one another.

In summary, the morphological, flotation gradient, and density-shift data presented above indicate that membrane and fluid markers are internalized into a shared endosomal compartment from which pIgR-IgA complexes are sorted. By convention, we define this sorting compartment as the AEE. Although the distribution of cell-associated FITC-dextran remained unchanged, pIgR-IgA was delivered to small vesicles that accumulated subapically. In this report, we define this downstream subapical compartment as the ARE.

### ***EEA1 Is Localized to the AEE, Whereas the Pericentriolar ARE Is Rab11 Positive***

The next series of experiments focused on establishing the biochemical identities of the compartments in which recycling IgA was observed. It has been observed that Rab5 is associated with the early endosomes of MDCK cells (Bucci *et*

*al.*, 1994). We have used an antibody that specifically recognizes the early endosomal antigen EEA1. EEA1 is an effector of Rab5 function and is localized to Rab5-positive compartments (Simonsen *et al.*, 1998). To label the AEE, IgA was internalized from the apical pole of the cell for 2.5 min at 37°C, and the samples were then costained for IgA and EEA1. EEA1 was localized to large vesicular structures that were occasionally found at the base of the cell and along the lateral margins of the cell. The majority of EEA1-positive structures were found in the apical cytoplasm of the cell in a supranuclear position (Figure 3E), but they were not abundant in the most subapical sections (Figure 3B). Many of the EEA1-positive structures overlapped with apically internalized IgA (Figure 3, C and F). However, there were IgA-positive puncta that did not colocalize with the EEA1. The identities of these compartments are unknown, but some of them could represent IgA in transit to the ARE or CE.

We confirmed, but do not show, that AEE labeled with FITC-dextran (internalized from the apical pole of the cell for 10 min at 37°C) show extensive colocalization with EEA1. When a 2.5-min pulse of IgA was chased into the ARE (by incubating for 7.5 min in the absence of ligand), there was little colocalization of the subapical IgA-containing endosomes and EEA1 (Figure 3I). In the supranuclear sections, there were larger IgA-labeled vesicular structures that colocalized with EEA1 and smaller structures that did not (Figure 3L). These observations show that a subset of the IgA-labeled AEE colocalizes with EEA1 but that the subapical IgA-labeled ARE elements do not colocalize with EEA1.

Recent evidence indicates that Rab11 may be a marker of recycling compartments, including the ARE (Ullrich *et al.*, 1996; Green *et al.*, 1997; Ren *et al.*, 1998; Casanova *et al.*, 1999). To determine if Rab11 was associated with the AEE or ARE, we colocalized Rab11 with IgA internalized for 2.5 min at 37°C, FITC-dextran internalized for 10 min at 37°C, EEA1, or IgA internalized for 10 min at 37°C. As described above, AEE labeled with a 2.5-min pulse of IgA were found in a supranuclear distribution (Figure 4D) and were largely excluded from the apical-most sections (Figure 4A). In contrast, Rab11 was associated with fine punctate elements that accumulated under the apical plasma membrane in a centralized distribution (Figure 4B) and at the apical margins of the cell (Figure 4E). Rab11 was not found in sections directly above the nucleus or at the basolateral pole of the cell (see Figure 8G). The distribution of Rab11 that we report is similar to that described previously (Casanova *et al.*, 1999; Brown *et al.*, 2000). There was little colocalization of the AEE (labeled with a 2.5-min pulse of IgA) and the Rab11-positive compartment (Figure 4, C and F). Moreover, there was little colocalization of Rab11 and FITC-dextran internalized from the apical pole of the cell for 10 min at 37°C, or of Rab11 and the EEA1 (Figure 4, G–L). However, a small amount of the total Rab11 signal was associated with an occasional EEA1-positive endosome (Figure 4L).

Whereas there was little colocalization of Rab11 and IgA internalized for 2.5 min at 37°C, there was extensive colocalization of Rab11 and IgA internalized for 10 min at 37°C (conditions under which large amounts of the IgA are present in the ARE). Both IgA and Rab11 were observed in the fine centralized array of subapical vesicles (Figure 5, A–C). The extensive colocalization extended to deeper sections as well (Figure 5, D–F). Similar results were observed

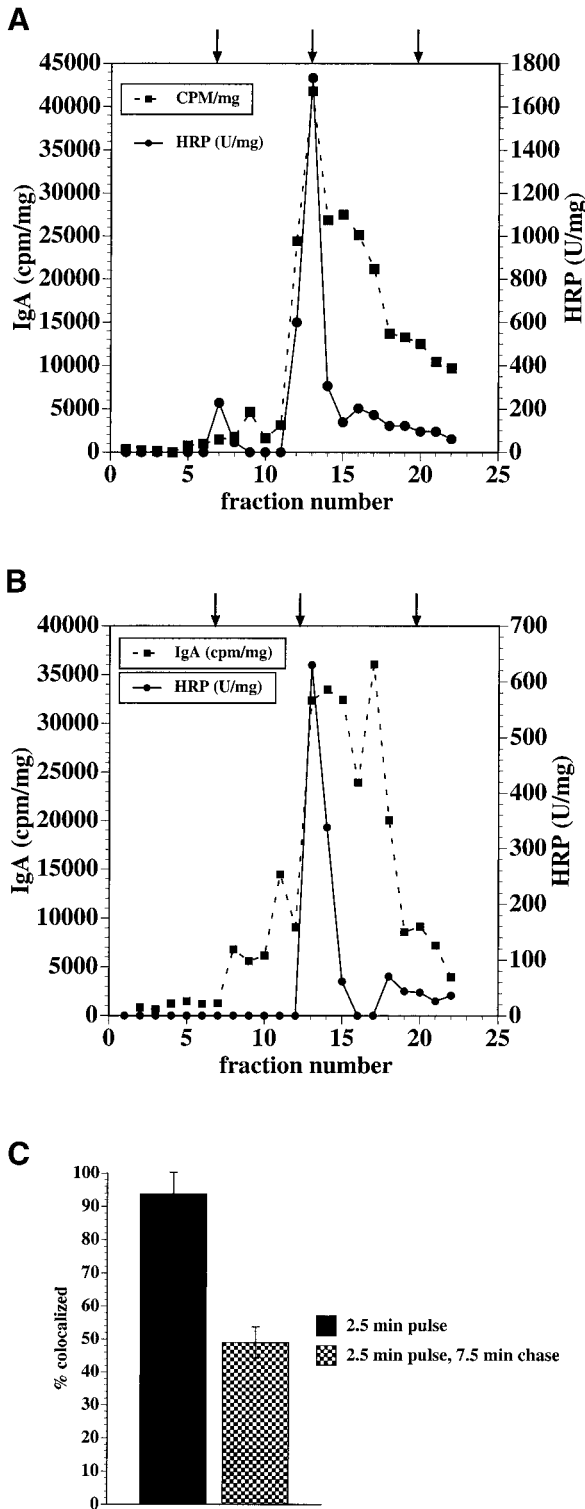


**Figure 2.** Colocalization of fluid and membrane markers assessed by sucrose flotation gradients and by density-shift assays. (A and B) Sucrose flotation gradients. [<sup>125</sup>I]IgA and 5 mg/ml HRP were coin-internalized for 2.5 min at 37°C from the apical poles of MDCK cells, and the cells were either rapidly chilled (A) or chased in marker-free

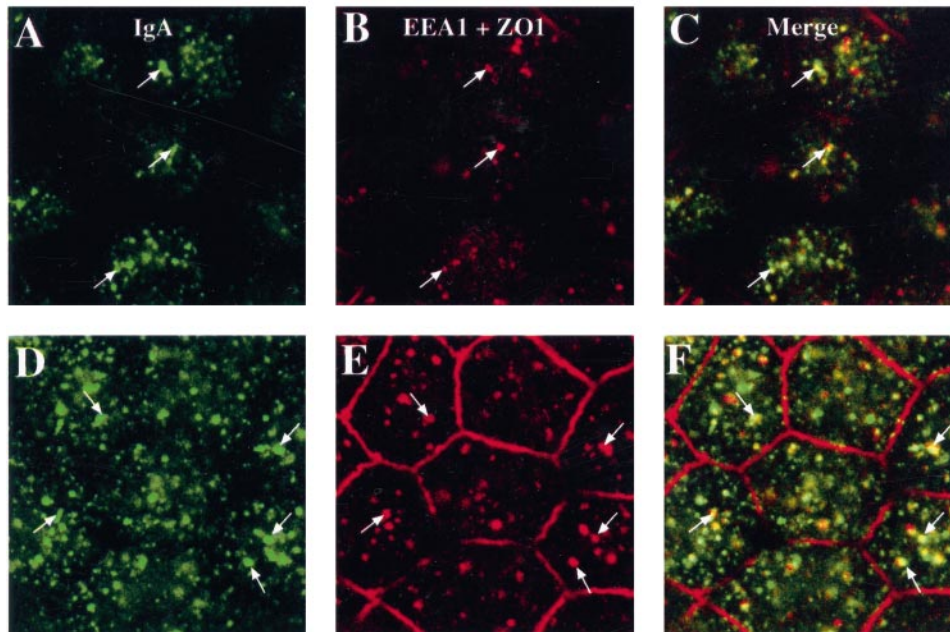
when the distribution of Rab11 was compared with that of IgA pulsed for 2.5 min at 37°C and chased for 7.5 min at 37°C. To confirm that Rab11 and recycling IgA were colocalized, we examined the distribution of IgA conjugated to HRP (internalized for 10 min at 37°C) and Rab11 by electron microscopy. The electron-dense reaction product produced by the IgA-HRP was observed in short tubules, vesicles, and signet-ring elements that accumulated directly under the apical pole of the cell (Figure 5G). The morphology and distribution of these elements is similar to our previous characterization of ARE elements (Apodaca *et al.*, 1994). Many of these IgA-HRP-labeled endosomes colocalized with Rab11 (identified with the use of 5-nm gold; arrows in Figure 5G). However, there were some Rab11-positive elements that were unlabeled with IgA-HRP (arrowheads in Figure 5G). The nature of these endosomes is unknown. Nonspecific gold labeling of mitochondria or the nuclear membrane was not observed, nor was gold label associated with structures at the basolateral pole of the cell. Finally, no gold labeling was observed if the primary anti-Rab11 antibody was omitted in the staining protocol. These observations indicate that the Rab11 compartment is distinct from the AEE and is a reasonable marker of the recycling endosome through which IgA passes en route to the apical plasma membrane.

**Entry into the Rab11 Positive Compartment Requires an Intact Microtubule Cytoskeleton**

We observed previously that the distribution of the ARE is altered in cells treated with the microtubule-depolymerizing agent nocodazole (Apodaca *et al.*, 1994). To determine if disruption of the microtubule cytoskeleton altered traffic from the AEE to the ARE, we performed the following experiments. IgA and FITC-dextran were internalized from the apical poles of nocodazole- or mock-treated cells for 10 min at 37°C. In mock-treated cells, IgA was found in the subapical elements of the ARE as well as in larger supranuclear vesicles. As described above, the IgA present in the supranuclear vesicles colocalized with FITC-dextran (Figure 6, D-F). In contrast, in cells treated with nocodazole, there

**Figure 2 (cont).** medium for 7.5 min at 37°C (B). The cells were homogenized, a postnuclear supernatant was generated, and the postnuclear supernatant (adjusted to 40.2% sucrose) was overlaid with 35, 25, and 8.5% (wt/wt) sucrose solutions. The samples were centrifuged, and 0.45-ml fractions were collected from the top of the gradient. Samples of each fraction were assayed for protein content, associated [<sup>125</sup>I]IgA (cpm), and HRP activity. The interfaces between the 40.2 and 35% sucrose layers, the 35 and 25% sucrose layers, and the 25 and 8.5% sucrose layers are indicated, from right to left, by arrows atop the panels. Data from a representative experiment are shown. (C) Density-shift assay. [<sup>125</sup>I]IgA and 5 mg/ml HRP were coin-internalized for 2.5 min at 37°C from the apical poles of MDCK cells, and the cells were either rapidly chilled or chased in marker-free medium for 7.5 min at 37°C. Cell surface [<sup>125</sup>I]IgA was removed by trypsin treatment at 4°C. A DAB reaction was performed, cells were lysed in detergent, and the lysates were centrifuged. Details of the quantitation are given in MATERIALS AND METHODS. Results are mean ± SD (n ≥ 3).

## IgA 2.5' Ap and EEA1



## IgA 2.5' Ap → 7.5' chase and EEA1

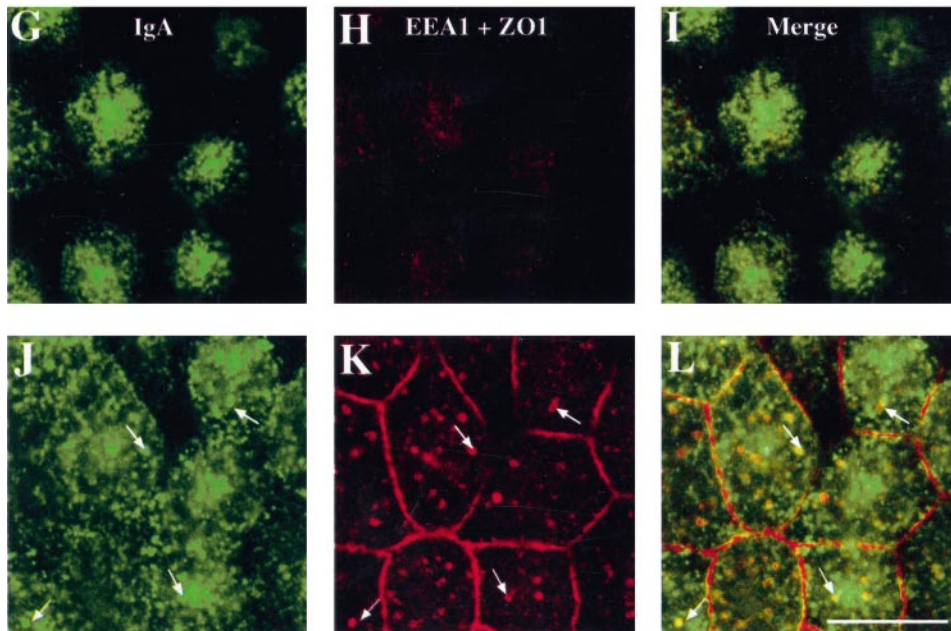
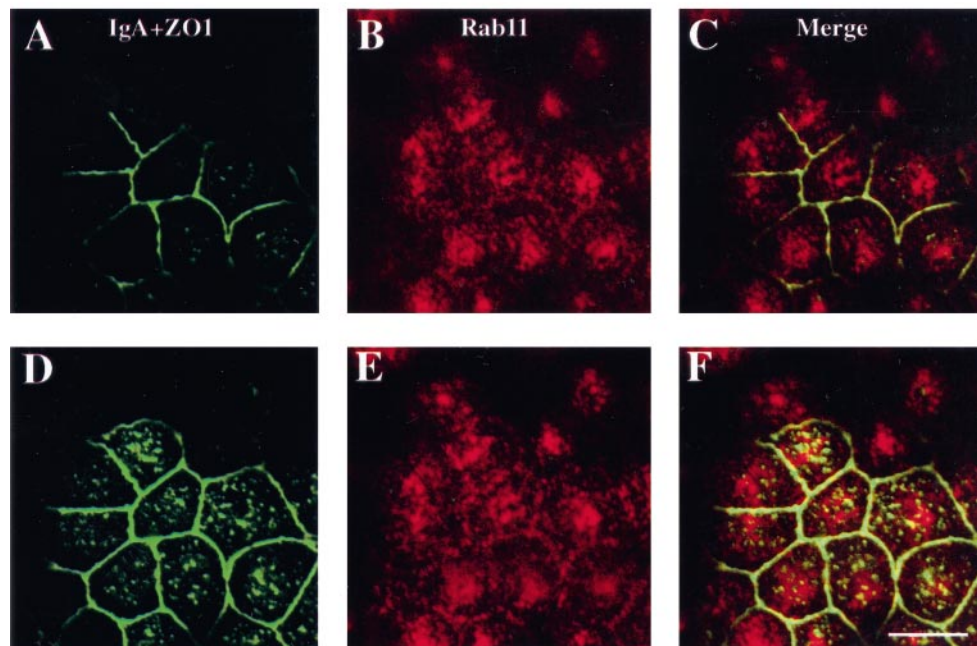


**Figure 3.** Distribution of EEA1 and apically internalized IgA in polarized MDCK cells. IgA was internalized for 2.5 min at 37°C from the apical poles of MDCK cells, and the cells were either rapidly chilled (A–F) or chased in marker-free medium for 7.5 min at 37°C (G–L). After IgA internalization, the cells were rapidly cooled, cell surface IgA was removed by trypsin treatment, and the cells were fixed with the use of a pH-shift protocol. The fixed cells were incubated with primary antibodies directed against IgA, ZO1, or EEA1 and then reacted with either FITC- or CY5-labeled secondary antibodies. The FITC signal is shown in the left panels, the CY5 signal is shown in the center panels, and merged images of the FITC and CY5 signals are shown in the right panels. ZO1 appears as a thin red line at the periphery of each cell. Single optical sections, obtained with a confocal microscope, are shown from the apex of the cell (A–C and G–I) or at the level of the tight junctions (D–F and J–L). Representative regions of colocalization are marked with arrows. Bar, 10  $\mu\text{m}$ .



## IgA 2.5' Ap and Rab11



## Rab11 and EEA1

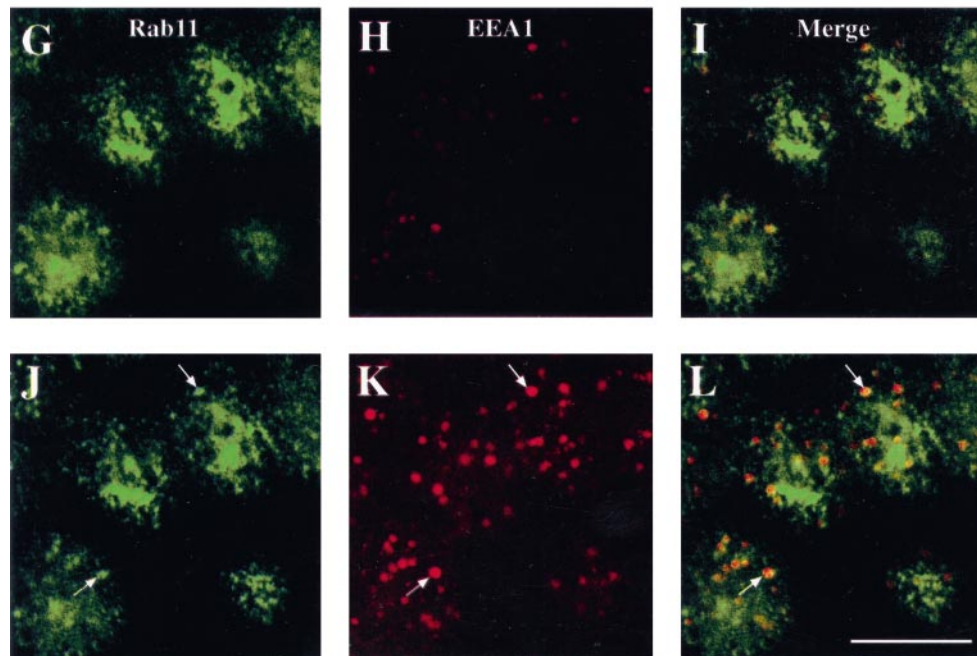


**Figure 4.** Distribution of IgA-labeled AEE, Rab11, and EEA1 in polarized MDCK cells. (A–F) IgA was internalized for 2.5 min at 37°C from the apical poles of MDCK cells. The cells were then rapidly chilled, cell surface IgA was removed by trypsin treatment, and the cells were fixed with the use of a pH-shift protocol. (G–L) Cells were immediately fixed. In A–L, the fixed cells were incubated with primary antibodies directed against IgA, Rab11, ZO1, or EEA1 and then reacted with either FITC- or CY5-labeled secondary antibodies. The FITC signal is shown in the left panels, the CY5 signal is shown in the center panels, and merged images of the FITC and CY5 signals are shown in the right panels. In A–F, ZO1 appears as a thin green line at the periphery of each cell. Single optical sections, obtained with a confocal microscope, are shown from the apex of the cell (A–C and G–I) or at or near the level of the tight junctions (D–F and J–L). Representative regions of colocalization are marked with arrows. Bars, 10  $\mu$ m.

## IgA 10.0' Ap and Rab11

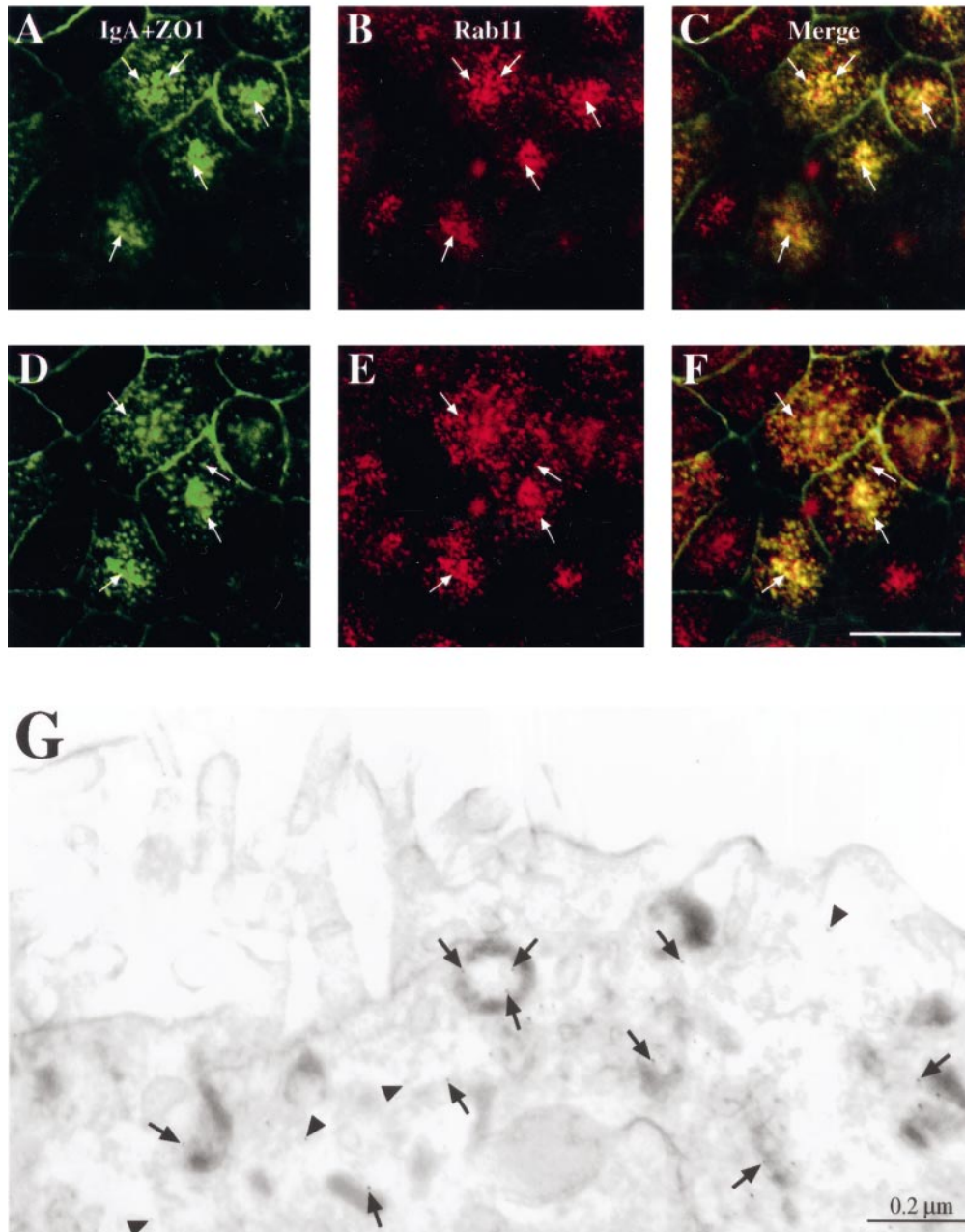
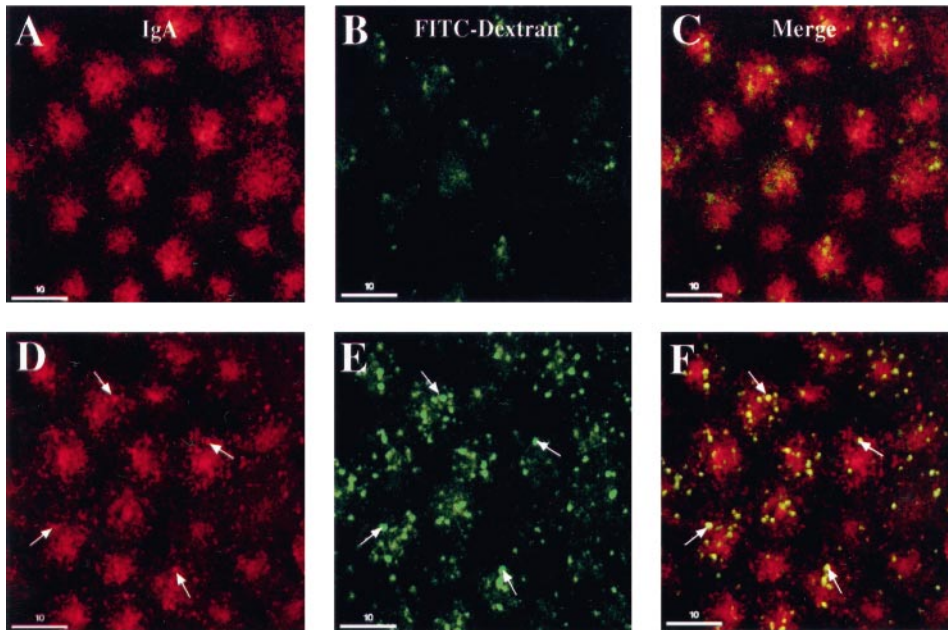


**Figure 5.** Distribution of IgA and Rab11 in polarized MDCK cells. (A–F) IgA was internalized from the apical poles of MDCK cells for 10 min at 37°C. The cells were then rapidly chilled, cell surface IgA was removed by trypsin treatment, and the cells were fixed with the use of a pH-shift protocol. The fixed cells were incubated with primary antibodies directed against IgA, Rab11, or ZO1 and then reacted with either FITC- or CY5-labeled secondary antibodies. The FITC signal is shown in the left panels, the CY5 signal is shown in the center panels, and merged images of the FITC and CY5 signals are shown in the right panels. ZO1 appears as a thin green line at the periphery of each cell. Single optical sections,  $\sim 1 \mu\text{m}$  apart, are shown from the apical region of the cell. Representative regions of colocalization are marked with arrows. Bar, 10  $\mu\text{m}$ . (G) IgA-HRP was internalized from the apical poles of the cells for 10 min at 37°C, the cells were fixed with the use of a pH-shift protocol, and a DAB reaction was performed. The cells were permeabilized with digitonin and then reacted with anti-Rab11 antibodies, followed by protein A coupled to 5-nm colloidal gold particles. The cells were then processed for electron microscopy as described in MATERIALS AND METHODS. A semithick section ( $\sim 250 \text{ nm}$ ) is shown. Arrows, examples of structures in which IgA-HRP and Rab11 colocalize; arrowheads, examples of areas in which Rab11 is found in the absence of IgA-HRP. Bar, 0.2  $\mu\text{m}$ .

60' 4° C → IgA + FITC-Dextran 10.0'



Noc 60' 4° C → IgA + FITC-Dextran 10.0' + Noc

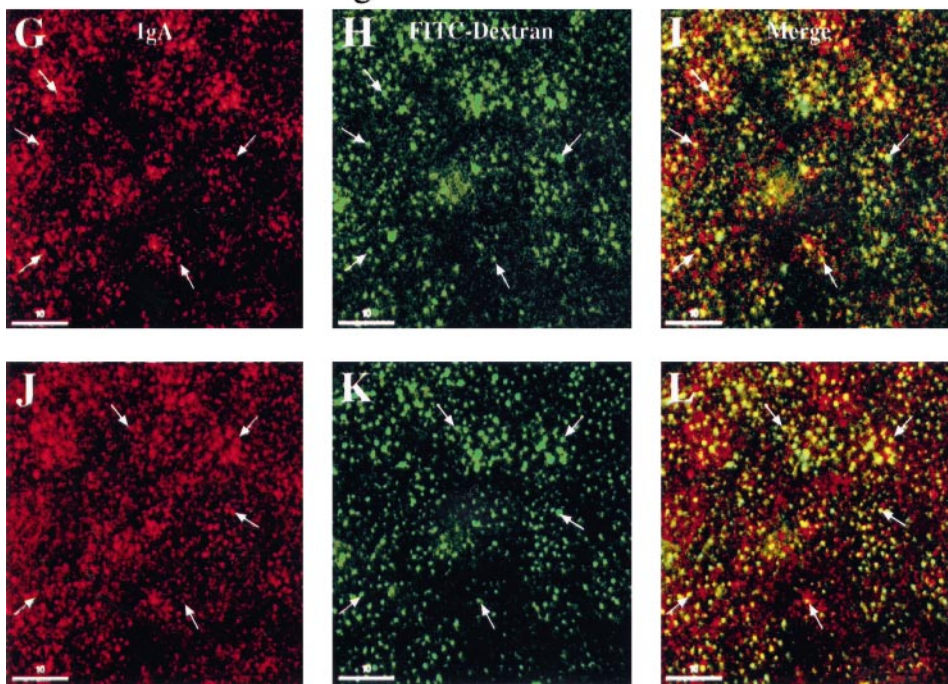


**Figure 6.** Distribution of IgA and FITC-dextran in control and nocodazole-treated cells. (A–F) Cells were incubated for 60 min at 4°C, and IgA and FITC-dextran were cointernalized for 10 min at 37°C from the apical poles of MDCK cells. (G–L) Cells were treated with nocodazole for 60 min at 4°C, and IgA and FITC-dextran were cointernalized (in the continued presence of nocodazole) from the apical poles of the cells for 10 min at 37°C. In A–L, the cells were rapidly chilled, cell surface IgA was removed by trypsin treatment, and the cells were fixed with the use of a periodate-lysine-paraformaldehyde fixative. The fixed cells were incubated with primary antibodies directed against IgA and then reacted with CY5-labeled secondary antibodies. The CY5 signal is shown in the left panels, the FITC signal is shown in the center panels, and merged images of the CY5 and FITC signals are shown in the right panels. Single optical sections, obtained with a confocal microscope, are shown from the apex of the cell (A–C and G–I) or 1–2 μm below the level of the previous section (D–F and J–L). Representative regions of colocalization are marked with arrows. Bars, 10 μm.

was extensive colocalization of the FITC-dextran and IgA in large vesicular structures that appeared randomly distributed in the apical cytoplasm (Figure 6, I and L). We noticed that more FITC-dextran accumulated in cells treated with nocodazole. We believe that this may reflect the slower exit of markers from the AEE, in part as the result of inhibition of fluid transport along the degradative pathway. There were some IgA-positive vesicles that were not dextran positive. These could be IgA-containing vesicles that were sorted from the dextran-positive AEE and were in the process of recycling. To quantify these observations, we measured the extent of HRP and [<sup>125</sup>I]IgA colocalization in mock- and nocodazole-treated cells with the use of the density-shift assay described above. After cointernalization (for 10 min at 37°C), we observed that 47.4 ± 7.2% of the IgA colocalized with HRP in mock-treated cells, whereas 88.2 ± 7.1% of the IgA colocalized with the HRP maker in nocodazole-pretreated cells.

These results indicate that either nocodazole treatment prevented efficient exit of IgA from the AEE or it caused the ARE elements to collapse into the AEE. To distinguish between these two possibilities, IgA was internalized for 10 min at 37°C from the apical poles of nocodazole-treated cells and the distribution of IgA and Rab11 was examined by confocal microscopy. We observed that there was little colocalization of IgA and Rab11, indicating that the Rab11-positive ARE elements had not collapsed into the AEE, and instead remained distinct (Figure 7, C and F). If, however, IgA was internalized first and then cells were treated with nocodazole, there was significant colocalization of Rab11 and IgA (Figure 7, I and L). The results are consistent with the AEE being distinct from the ARE and confirm that delivery of IgA from the AEE to the ARE requires microtubules.

#### ***The Rab11-positive Compartment Is Distinct from the Tf-rich CE***

We next examined the relationship of the Tf-rich CE and the EEA1-positive AEE or Rab11-positive ARE. Initially, we determined whether Tf and Rab11 colocalized. In fact, Tf was largely excluded from the apical-most sections of the cell (Figure 8B), the sections in which maximal staining of Rab11 was observed (Figure 8A). Even in supranuclear sections, little colocalization was observed between Rab11 and the large supranuclear Tf-rich endosomal elements (the rare regions of colocalization are noted in Figure 8F). Although Tf-labeled endosomes were found in abundance just above the nucleus (Figure 8H), little Rab11 was found in this region of the cell (Figure 8H).

We also determined if Tf colocalized with IgA-labeled ARE elements (labeled by pulsing with ligand for 2.5 min followed by a 7.5-min chase). Although little colocalization was observed between IgA and Tf in the fine vesicular puncta at the apex of the cell (Figure 9C), some colocalization was observed between Tf and IgA in the large supranuclear structures that were deeper in the apical cytoplasm (Figure 9F). These large supranuclear IgA- and Tf-positive vesicles were similar to the AEE elements described above.

To determine if Tf was present in AEE, we analyzed the distribution of IgA-labeled AEE and Tf (Figure 10). The relationship of these markers and Rab11 was also assessed. Significant colocalization between IgA (internalized from

the apical pole of the cell for 2.5 min at 37°C) and basolaterally internalized Tf was observed (Figure 10, F–H and J–L, arrows). These data indicate that Tf had access to the AEE. We also observed that Tf colocalized to some extent with apically internalized FITC-dextran, again confirming that Tf had access to the AEE. There were Tf-labeled endosomes that did not overlap the AEE marker, and these were found in supranuclear sections (Figure 10H) and in sections directly above the nucleus (Figure 10L). These presumably represent elements of the Tf-rich CE. Tf was also found along the lateral margins of the cell (Figure 10P) and at the base of the cell. As described above, the staining of the Tf-labeled structures or the IgA-labeled AEE did not overlap that of the Rab11-positive ARE elements (Figure 10, D and H). Because localization of Tf with apically internalized fluid-phase marker was surprising, we confirmed this finding biochemically with the use of the density-shift assay described above. When [<sup>125</sup>I]Tf was internalized basolaterally and fluid-phase HRP was cointernalized from the apical pole of the cell, colocalization of these two markers was observed. However, the percentage of total internalized Tf present in the HRP-labeled AEE was modest (11.8 ± 1.9%).

## **DISCUSSION**

Understanding how polarized membrane domains are established and maintained requires an intimate knowledge of the membrane and solute trafficking pathways of the cell, the sites of sorting, and the mechanisms used to acutely and developmentally regulate these pathways. Past attempts at delineating the endocytic pathways of polarized cells were complicated by the use of either fluid or membrane markers, lack of agreement on what to call the labeled compartments, disagreements on the sites of sorting, and lack of compartment-specific markers (Bomsel *et al.*, 1989; Parton *et al.*, 1989; Apodaca *et al.*, 1994; Barroso and Sztul, 1994; Knight *et al.*, 1995; Odorizzi *et al.*, 1996; Sheff *et al.*, 1999).

#### ***Sorting at the Apical Poles of Polarized MDCK Cells***

We have carefully analyzed the pathways used by fluid and membrane markers at the apical pole of the MDCK cell and have defined potential sites for sorting and recycling. Moreover, we have identified markers that are associated with these compartments. We find that when fluid-phase FITC-dextran and receptor-bound IgA (a membrane marker) are cointernalized for short periods of time they are delivered to an apically distributed endosomal compartment, where they colocalize, and are then rapidly sorted from one another. Morphologically, this early compartment is composed of relatively large vesicles that primarily reside in a supranuclear position. Because of its location, rapid filling with endocytosed fluid and membrane, and putative role in sorting, we refer to this compartment as the AEE. Moreover, EEA1, an antigen associated with early endosomes, is also localized to this compartment (see below).

Although FITC-dextran (internalized from the apical pole of the cell for up to 10 min at 37°C) is detected only in the AEE, a significant fraction of internalized IgA is delivered to a downstream “recycling” compartment composed of fine vesicular elements. Many of these small vesicles are in the

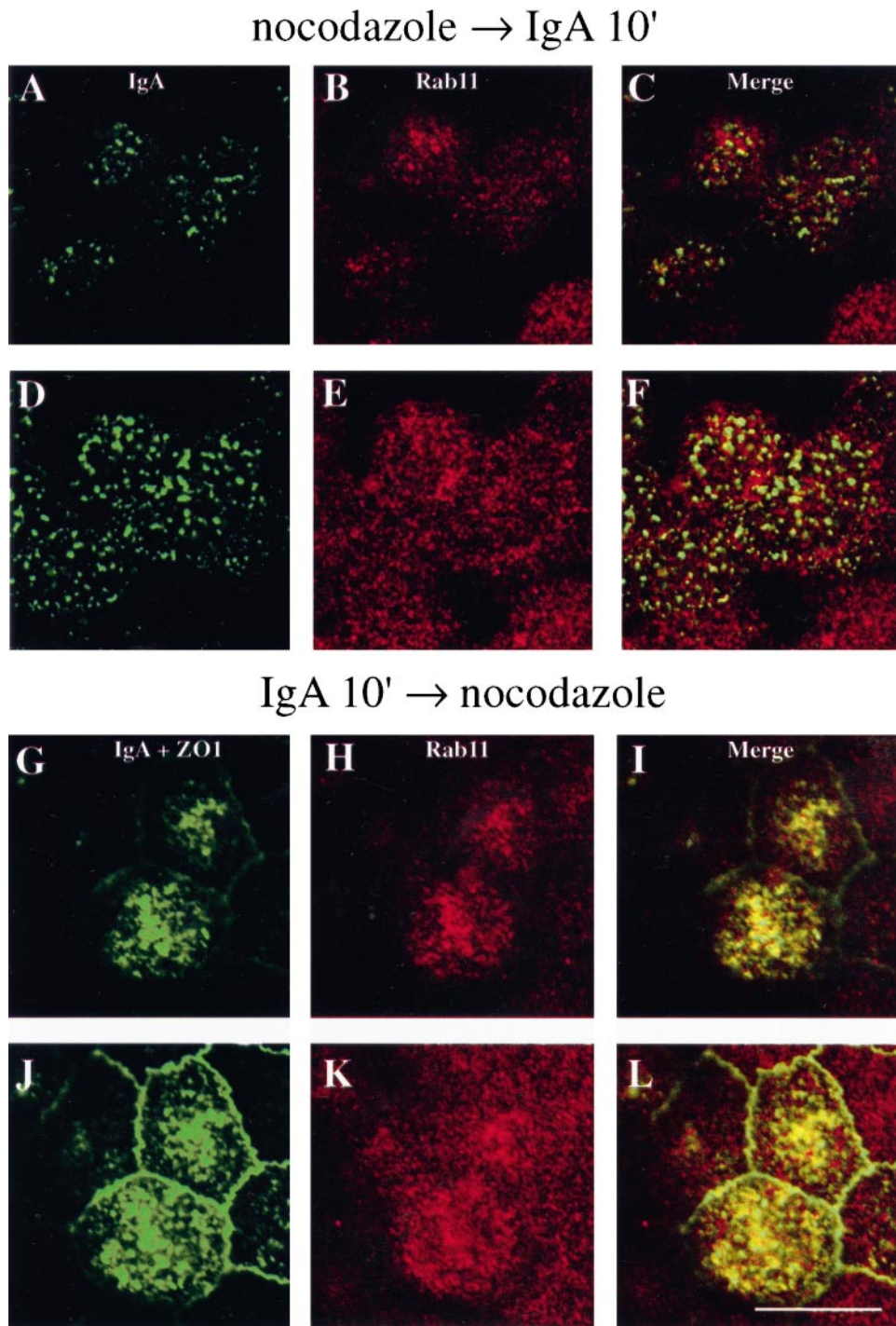


**Figure 7.** Distribution of Rab11 and IgA in nocodazole-treated cells. (A–F) Cells were treated with nocodazole for 60 min at 4°C and then for 10 min at 37°C. Subsequently, IgA and FITC-dextran were cointernalized from the apical poles of MDCK cells for 10 min at 37°C in the continued presence of nocodazole. (G–L) IgA was internalized from the apical poles of the cells for 10 min at 37°C. The cells were then rapidly chilled, treated with nocodazole for 60 min at 4°C, and warmed for 10 min at 37°C in the continued presence of nocodazole. In A–L, the cells were rapidly chilled, cell surface IgA was removed by trypsin treatment, and the cells were fixed with the use of a pH-shift protocol. The fixed cells were incubated with primary antibodies directed against IgA, Rab11, or ZO1 and then reacted with FITC- or CY5-labeled secondary antibodies. The FITC signal is shown in the left panels, the CY5 signal is shown in the center panels, and merged images of the FITC and CY5 signals are shown in the right panels. In G–L, ZO1 appears as a thin green line that surrounds each cell. Single optical sections, obtained with a confocal microscope, are shown from the apex of the cell (A–C and G–I) or at or near the level of the tight junctions (D–F and J–L). Bar, 10  $\mu$ m.

## Tf and Rab11

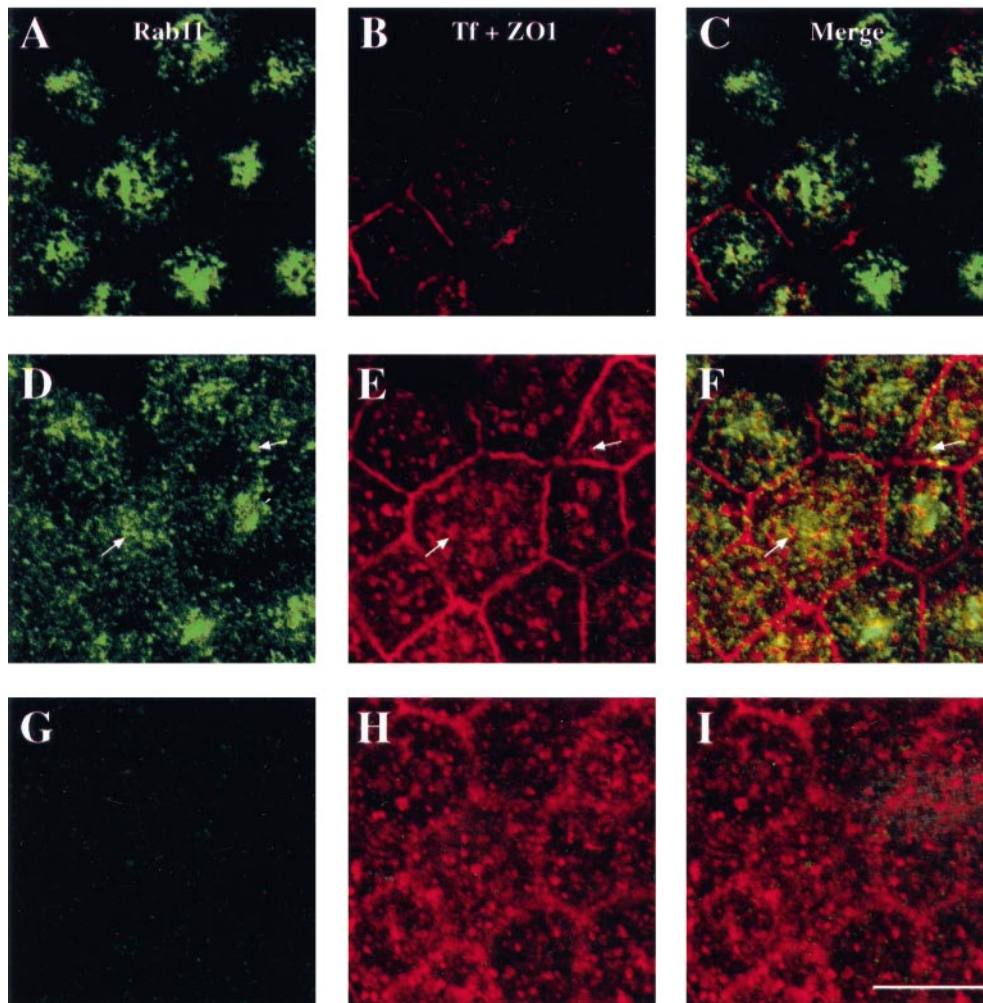


**Figure 8.** Distribution of Tf and Rab11 in polarized MDCK cells. Tf was internalized from the basolateral poles of the cells for 30 min at 37°C. The cells were fixed, incubated with primary antibodies directed against Rab11, ZO1, or Tf, and then reacted with either CY5- or FITC-labeled secondary antibodies. The FITC signal is shown in the left panels, the CY5 signal is shown in the center panels, and merged images of the FITC and CY5 signals are shown in the right panels. ZO1 appears as a thin red line at the periphery of each cell. Single optical sections, obtained with a confocal microscope, are shown from the apex of the cell (A–C), at or near the level of the tight junctions (D–F), or directly above the nucleus (G–I). Representative regions of colocalization are marked with arrows. Bar, 10  $\mu\text{m}$ .

same plane as the AEE, whereas the majority of them are found to accumulate directly under the apical plasma membrane in a pericentriolar subapical distribution. This morphological finding was confirmed by cell-fractionation and density-shift assays. By convention, we refer to this downstream subapical compartment as the ARE; it is apically distributed and receives apical recycling IgA from an upstream sorting compartment. Like many recycling compartments, the ARE is Rab11 positive (Ullrich *et al.*, 1996; Green *et al.*, 1997; Chen *et al.*, 1998; Ren *et al.*, 1998; Casanova *et al.*, 1999). As described below, some of the IgA may be delivered from the AEE to the CE. We note that the definition of ARE used in this report is more restrictive than that used in our previous work, in which we defined ARE as the endosomal compartment labeled with a 10-min pulse of an apically

internalized membrane marker (Apodaca *et al.*, 1994). As originally defined, the ARE would also include the AEE and perhaps elements of the CE.

The mechanism of membrane and fluid sorting is unknown but might reflect the geometries of sorting endosomes. Membranous markers are thought to partition with the tubular aspects of the sorting endosome, whereas fluid is retained in the volume-rich vesicular portions of the endosome (reviewed by Mukherjee *et al.*, 1997). By budding off the tubular portions of these endosomes in an iterative process, it is possible to achieve high-fidelity sorting of membrane and fluid (Dunn *et al.*, 1989). In addition to sorting apical recycling molecules from fluid-phase molecules, we also observed that basolateral recycling Tf was delivered to the AEE. This was a surprising observation because it has

## IgA 2.5' → 7.5' chase and Tf BI

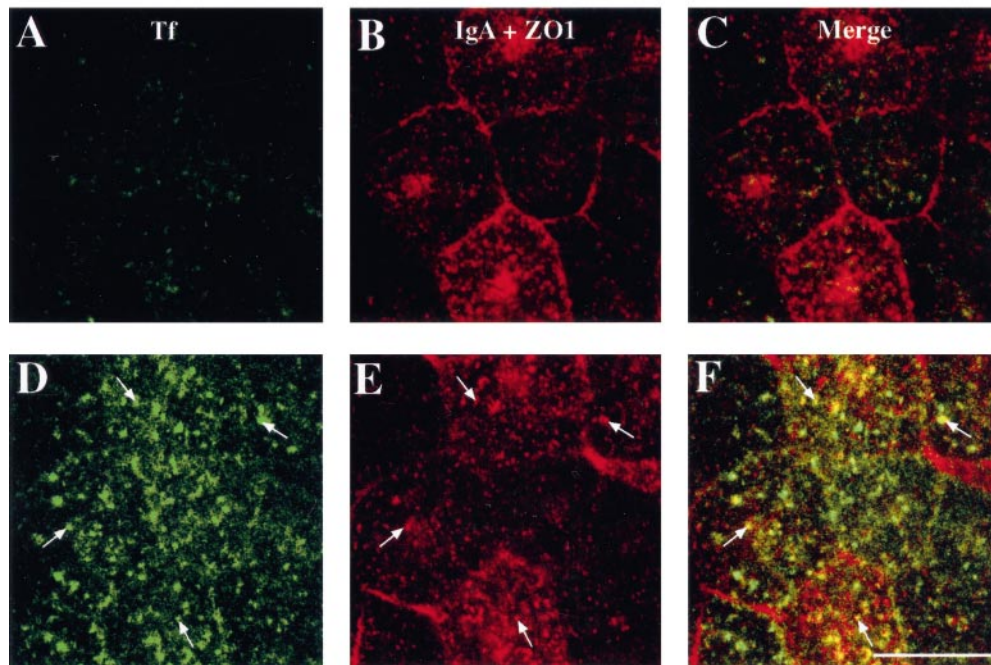


**Figure 9.** Distribution of Tf and IgA. IgA was internalized from the apical poles of the cells for 2.5 min at 37°C and then incubated in marker-free medium for 7.5 min at 37°C. The cells were rapidly chilled, cell surface IgA was removed by trypsin treatment, and the cells were fixed with the use of a pH-shift protocol. The fixed cells were incubated with primary antibodies directed against IgA, ZO1, or Tf and then reacted with either CY5- or FITC-labeled secondary antibodies. The FITC signal is shown in the left panels, the CY5 signal is shown in the center panels, and merged images of the FITC and CY5 signals are shown in the right panels. ZO1 appears as a thin red line at the periphery of each cell. Optical sections are shown from the apical region of the cell just below the apical plasma membrane (A–C) or in sections near the level of the tight junctions (D–F). Representative regions of colocalization are marked with arrows. Bar, 10  $\mu\text{m}$ .

not been shown previously that apically internalized fluid-phase markers mix with basolaterally internalized Tf. In fact, the presence of basolaterally internalized Tf and apical recycling IgA in this compartment suggests that it may be a subdomain of the CE (Odorizzi *et al.*, 1996). If so, the AEE may also play a role in the recycling of basolaterally internalized proteins. Recycling may be via 60-nm vesicles that are coated with AP1 adaptor complexes (Futter *et al.*, 1998). An alternative possibility is that the Tf found in the AEE is en route to the apical plasma membrane; ~5% of Tf is transcytosed and released at the apical pole of the cell (Fuller and Simons, 1986). This may explain why only a small fraction of the total cellular Tf colocalizes with HRP-labeled AEE in the density-shift assays.

Although our present results, and those of others, do not rule out the possibility that some sorting may occur in the ARE, they do suggest that much of the sorting of fluid and basolateral recycling markers occurs in compartments upstream of the ARE (e.g., in the AEE or CE). There is evidence that in hepatocytes sorting of membrane markers occurs in the so-called subapical compartment (van IJzendoorn *et al.*, 1997; Ihrke *et al.*, 1998; van IJzendoorn and Hoekstra, 1998). The relationships of the AEE and ARE with this compartment are unclear, although they are likely to be related. In fact, the distribution of the hepatocyte subapical compartment and its lack of basolateral recycling markers suggest

that it may be composed in part of AEE- and/or ARE-like elements (Hemery *et al.*, 1996; Ihrke *et al.*, 1998; van IJzendoorn and Hoekstra, 1999). We previously suggested that the ARE is the polarized cell equivalent of the paracentriolar recycling endosome observed in nonpolarized cells (Apodaca *et al.*, 1994). This was based in part on the observations that both compartments are composed of tubular elements, are organized about the centrosome, and receive cargo from upstream compartments. It is apparent from our current analysis that the ARE is in fact depleted of Tf and is therefore distinct from the Tf-rich recycling endosome observed in nonpolarized cells.

#### Role for Microtubules in Delivery of Cargo to the ARE

In nonpolarized cells, the delivery of cargo from early endosomes to late endosomes requires an intact microtubule cytoskeleton (Gruenberg *et al.*, 1989). Likewise, in polarized cells, movement of cargo from the BEE to the apical pole of the cell requires microtubules (Hunziker *et al.*, 1990; Apodaca *et al.*, 1994; Brown *et al.*, 2000). We report that traffic between the AEE and the ARE is blocked in cells treated with nocodazole. It was reported previously that apical recycling of IgA is slowed in cells treated with nocodazole (Breitfeld *et al.*, 1990). That IgA recycling is not completely

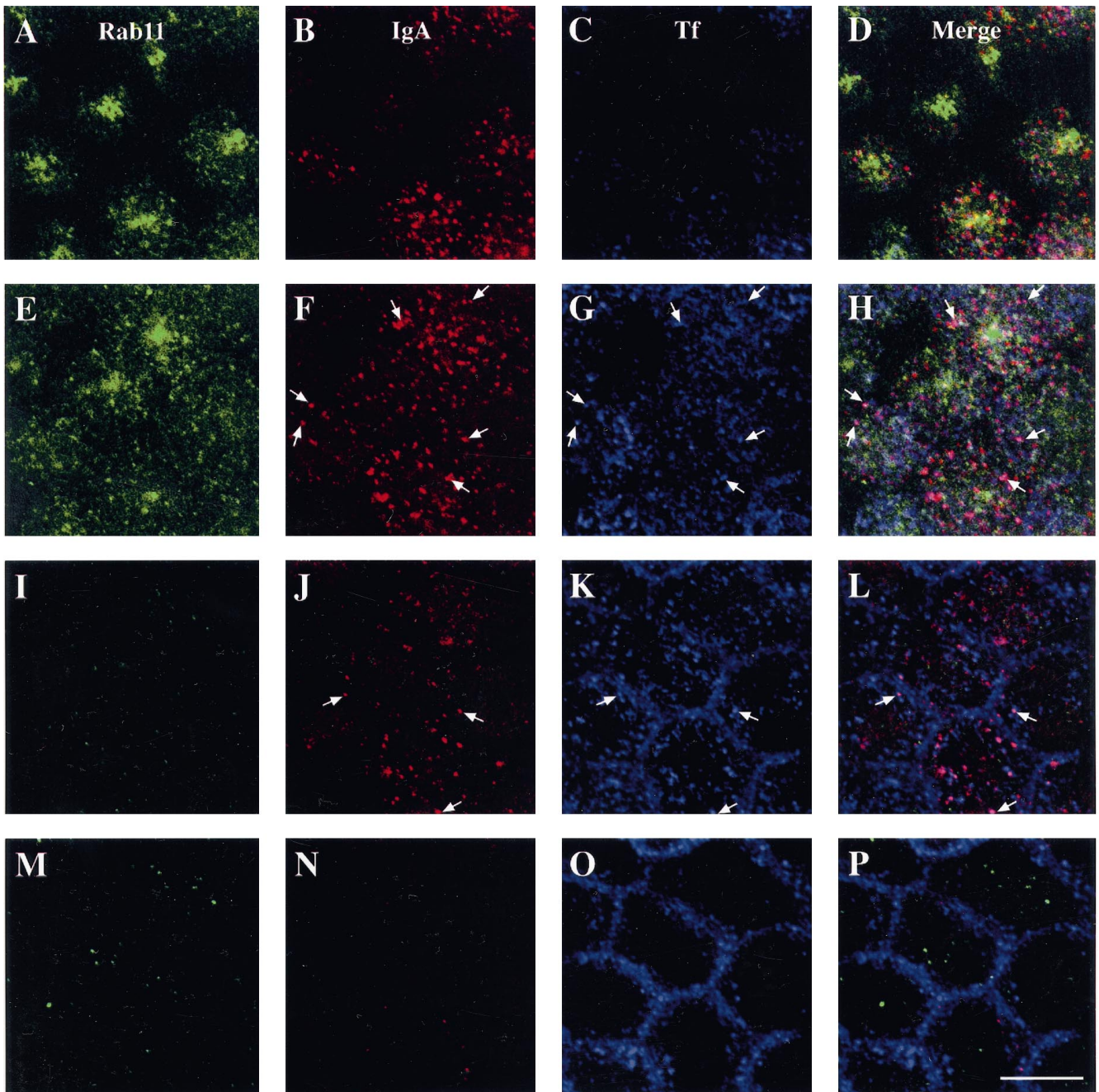


**Figure 10.** Distribution of Tf, IgA-labeled AEE, and Rab11 in polarized MDCK cells. Tf was internalized from the basolateral poles of the cells for 30 min at 37°C. During the last 2.5 min of this internalization period, IgA was added to the apical poles of the cells. At the end of the experiment, the cells were rapidly chilled, cell surface IgA was removed by trypsin treatment, and the cells were fixed with the use of a pH-shift protocol. The cells were incubated with primary antibodies directed against Rab11, IgA, or Tf and then reacted with either CY5-, CY3-, or FITC-labeled secondary antibodies. The FITC signal (in green) is shown in the left panels, the CY3 signal (in red) is shown in the center left panels, the CY5 signal (in blue) is shown in the center right panels, and merged images of the FITC, CY3, and CY5 signals are shown in the right panels. Single optical sections, obtained with a confocal microscope, are shown from the apex of the cell (A–D), at or near the level of the tight junctions (E–H), directly above the nucleus (I–L), or along the lateral margins of the cell near its base (M–P). Note that the cells in the lower right corner of each panel are taller than the cells in the upper left corner. Regions of colocalization of IgA and Tf appear magenta in the merged images, and representative regions of colocalization are indicated by arrows. Bar, 10  $\mu$ m.



inhibited by microtubule depolymerization indicates that passage through the ARE is not an obligatory step in the recycling process. In such cases, recycling may occur directly from the AEE or from some intermediate compartment. Similarly, recycling of Tf in nonpolarized cells is apparently unaffected by nocodazole treatment (McGraw *et al.*, 1993), possibly the result of direct recycling from early sorting endosomes, as was suggested recently (Sheff *et al.*, 1999). If cargo can recycle directly from early endosomes, why is cargo delivered to these recycling compartments at all? As described below, the primary function of recycling compartments such as the ARE may be to modulate traffic flow to the cell surface. In the case of polarized epithelial cells, traffic to and from the apical cell surface must be highly regulated to preserve normal cellular function and maintenance of a polarized phenotype (Mostov and Cardone, 1995).

### ***EEA1 Is Associated with the AEE and Rab11 Is Associated with the ARE***

One of the most difficult challenges facing cell biologists studying endocytic traffic in polarized epithelial cells has been to discriminate between the various endosomal subcompartments. In the present study, we have used antibodies that recognize endogenous EEA1 and Rab11. In MDCK cells, EEA1 is primarily associated with a population of large supranuclear vesicles in the apical cytoplasm of the cell. However, it is also found on the occasional basolateral vesicle. Notably, we observe that many of these supranuclear EEA1-positive vesicles receive membrane and fluid internalized from the apical pole of the cell for short pulses, consistent with these structures being AEE. The basolaterally distributed EEA1-positive vesicles are presumably performing a similar function at the basolateral pole of the cell. Although EEA1 is not associated exclusively with the AEE, it is a convenient marker to discriminate between markers in the AEE and those en route to or delivered to the ARE.

Our results further indicate that Rab11 may be a useful marker of the MDCK ARE. In nonpolarized cells, Rab11 is primarily associated with the recycling endosome and, to a lesser extent, with the *trans*-Golgi network (Ullrich *et al.*, 1996; Green *et al.*, 1997; Chen *et al.*, 1998; Ren *et al.*, 1998; Casanova *et al.*, 1999). We find no evidence that Rab11 is associated with the *trans*-Golgi network of polarized MDCK cells (our unpublished observations). Consistent with observations made in gastric parietal cells and recent reports in MDCK cells, we observe that Rab11 is associated with small tubular vesicles localized under the apical membrane (Goldring *et al.*, 1994; Casanova *et al.*, 1999; Brown *et al.*, 2000). In MDCK cells, these Rab11-positive endosomal elements receive apical recycling and transcytosing cargo from upstream sorting compartments (the AEE and CE, respectively) (Casanova *et al.*, 1999; Brown *et al.*, 2000; this work). We do not observe that endogenous Tf and Rab11 colocalize to any notable extent in polarized MDCK cells. It has been observed that Rab11 is associated with sucrose gradient fractions enriched in Tf-labeled recycling compartments (prepared from MDCK cells overexpressing the human Tf receptor) (Sheff *et al.*, 1999). However, consistent with our observations,  $\ll 1\%$  of the total cellular Rab11 was associated with these gradient fractions; the vast majority of Rab11 had dissociated from the membrane and was found in other fractions in the gradient (Sheff *et al.*, 1999). Moreover, colo-

calization of Rab11 and Tf has not been observed in nonpolarized MDCK cells (Brown *et al.*, 2000).

In addition to Rab11, there is evidence that Rab17 and Rab25 may be associated with the ARE or a subdomain of this compartment (Hunziker and Peters, 1998; Zacchi *et al.*, 1998; Casanova *et al.*, 1999). Rab25 labels a subapical compartment directly below the apical plasma membrane (Casanova *et al.*, 1999). Expression of a dominant active mutant of this protein slows transcytosis and apical recycling of IgA but has no effect on basolateral recycling of Tf (Casanova *et al.*, 1999). This result is consistent with our observation that Tf is largely excluded from the subapical elements of the ARE. There are light microscopy data that suggest that the distribution of Rab25 and Rab11 overlap significantly, but their distributions are not identical (Casanova *et al.*, 1999). The relationship of the Rab17 compartments with those associated with Rab25 and Rab11 has not been assessed. The presence of multiple Rabs with overlapping distribution on subapical elements suggests that the ARE may contain subdomains with specialized functions that remain to be described.

### ***Model for Sorting at the Apical Pole of Polarized MDCK Cells***

In summary, we propose the following model for endocytic traffic in polarized MDCK cells (Figure 11). Membrane and fluid, internalized from the apical pole of the cell, are rapidly delivered to the EEA1-positive AEE (Figure 11, step 1A). It is in this compartment that sorting of apical recycling and fluid-phase markers is thought to occur. Although apically internalized fluid is thought to primarily recycle or transcytose (Bomsel *et al.*, 1989), a fraction is delivered to late endosomes (step 2A) and ultimately to lysosomes (not shown). It is unclear at present if fluid markers recycle from the AEE or through the ARE. Because little fluid is observed in the ARE, it is likely that recycling occurs directly from the AEE (step 3A). Likewise, some membrane proteins may recycle directly from the AEE. However, a significant fraction of recycling membrane proteins are delivered to the Rab11-positive ARE (step 3B) or to the Tf-rich CE (step 3C). Delivery to the ARE apparently requires an intact microtubule cytoskeleton. The pathways taken by proteins transcytosing in the apical-to-basolateral direction (step 7) are not well understood, but they likely involve initial passage through the AEE.

In addition to receiving apical recycling proteins, the Rab11-, Rab17-, and Rab25-positive ARE also receives cargo transcytosing in the basolateral-to-apical direction (step 6A) (Apodaca *et al.*, 1994; Barroso and Sztul, 1994). The presence of multiple Rab proteins on this compartment indicates that it may be composed of multiple subcompartments with specialized function. Exit from the ARE (step 4) may be via C-shaped vesicles (Gibson *et al.*, 1998). Although the ARE may have some role in sorting, we suggest that one of its primary functions may be to fine tune or regulate endocytic traffic directed specifically toward the apical pole of the cell. In fact, there is evidence that multiple regulatory phenomena act at the level of the ARE. For example, ligand-stimulated transcytosis of basolaterally internalized pIgR and protein kinase C-stimulated transcytosis and apical recycling are thought to occur at the level of the ARE (Cardone *et al.*, 1994; Song *et al.*, 1994). Future studies will delineate the role

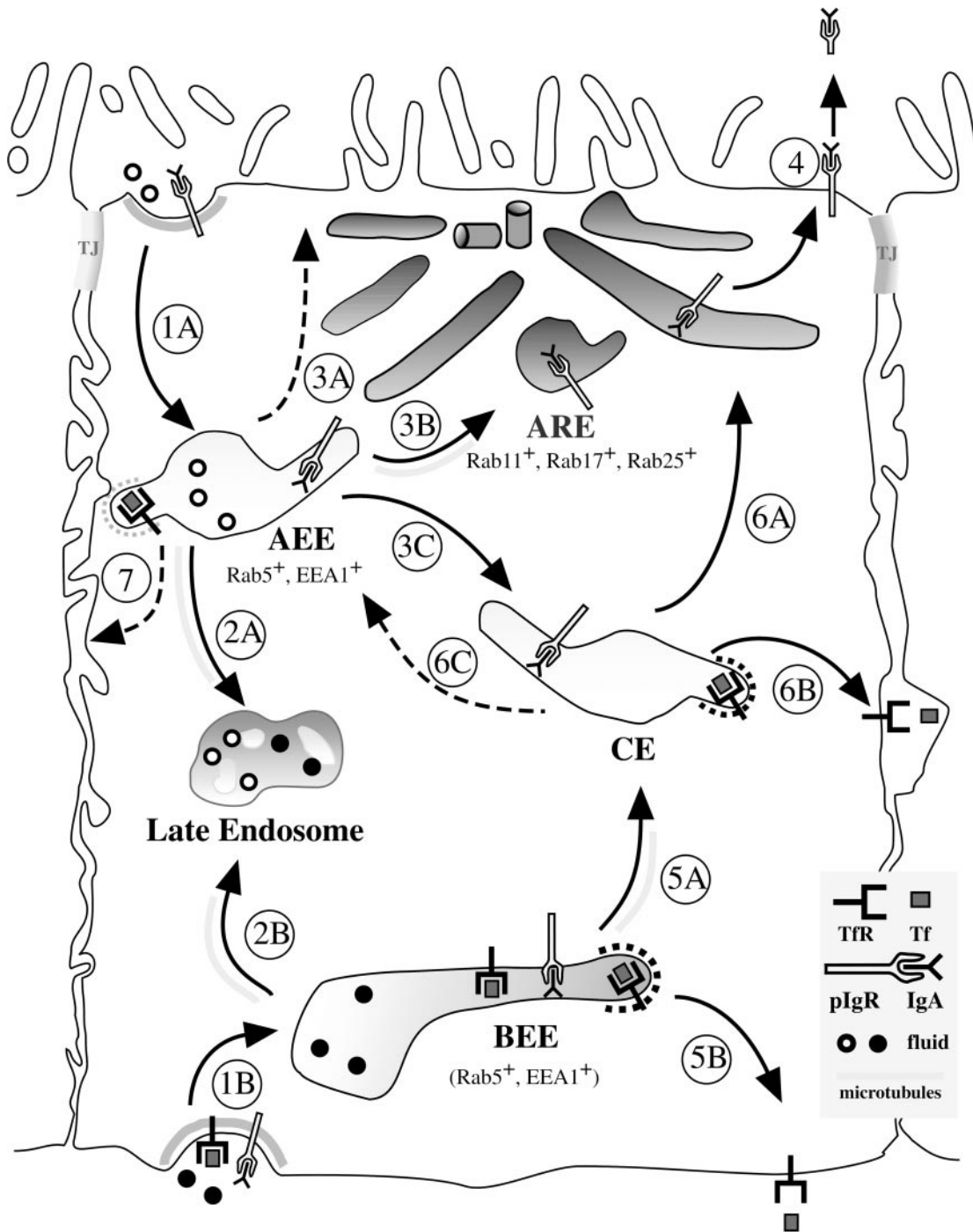


**Figure 11.** Model for endocytic traffic in polarized MDCK cells. Upon internalization, fluid and membrane are delivered to distinct AEE (step 1A) or BEE (step 1B). Although some fluid can recycle (step 3A) or transcytose (step 7) from these compartments, some is also delivered in a microtubule-dependent step to late endosomes (steps 2A and 2B) and ultimately lysosomes (not shown). Apical recycling proteins are delivered to the ARE (step 3B) or the CE (step 3C) before their ultimate release from the apical pole of the cell (step 4). Some membrane/fluid may recycle directly from the AEE (step 3A). Basolateral recycling proteins (i.e., receptor-bound Tf) as well as proteins transcytosing in the basolateral-to-apical direction (i.e., pIgR-IgA) enter a shared BEE (step 1B). Although some receptor-bound Tf may recycle directly from this compartment (step 5B), a significant fraction is delivered to the CE along with the majority of the pIgR-IgA (step 5A). This translocation step is thought to require microtubules. The majority of the receptor-bound Tf is thought to recycle from the CE (step 6B); however, a fraction is delivered to the AEE (step 6C) and may recycle from this compartment (step 7). The transcytosing pIgR-IgA complexes, as well as apical recycling pIgR-IgA complexes, are delivered from the CE to the ARE (step 6A) and are ultimately released at the apical pole of the cell (step 4).

of Rab11, Rab 17, and Rab25 in ARE subcompartmentalization and function.

The basolateral recycling marker Tf has access to multiple compartments, including the BEE, CE, and AEE. However, it is excluded from the ARE. Recycling of receptor-bound Tf may occur from the BEE (step 5B) as well as from the CE (step 6B) (Odorizzi *et al.*, 1996; Gibson *et al.*, 1998; Sheff *et al.*, 1999; Brown *et al.*, 2000). In addition, we observe that a small fraction of basolaterally internalized Tf has access to the AEE (step 6C). As such, the AEE may be a subdomain of the CE and may play a role in directing proteins to the basolateral pole of the cell (step 7). However, we cannot rule out the possibility that the small amount of Tf found in the AEE represents ligand-receptor complexes that are trafficking toward the apical plasma membrane. At present, it is difficult to define the boundaries of the CE because there are no specific markers for this compartment. It has been hypothesized recently that the newly described AP1-B adaptor complex may play a role in basolateral delivery of proteins from both the *trans*-Golgi network and endosomes (Fölsch *et al.*, 1999; Mostov *et al.*, 1999). By comparing the distribution of AEE and ARE markers with AP1-B-positive endosomes (labeled with Tf), the relationship of these compartments may become clarified. Our analysis is a first step in dissecting the complex endosomal sorting events and subcompartmentalization that occurs at the apical poles of polarized MDCK cells.

## ACKNOWLEDGMENTS

We thank Drs. O. Weisz, R. Hughey, and J. Smith for their insightful comments and critiques during the preparation of this report. This work was supported by grant RO1DK51970 from the National Institutes of Health to G.A. The Laboratory of Epithelial Biology is supported in part by an equipment grant from Dialysis Clinics Inc.

## REFERENCES

- Apodaca, G., Katz, L.A., and Mostov, K.E. (1994). Receptor-mediated transcytosis of IgA in MDCK cells is via apical recycling endosomes. *J. Cell Biol.* *125*, 67–86.
- Barroso, M., and Sztul, E. (1994). Basolateral to apical transcytosis in polarized cells is indirect and involves BFA and trimeric G protein sensitive passage through the apical endosome. *J. Cell Biol.* *124*, 83–100.
- Bomsel, M., Parton, R., Kuznetsov, S.A., Schroer, T.A., and Gruenberg, J. (1990). Microtubule- and motor-dependent fusion in vitro between apical and basolateral endocytic vesicles from MDCK cells. *Cell* *62*, 719–731.
- Bomsel, M., Prydz, K., Parton, R.G., Gruenberg, J., and Simons, K. (1989). Endocytosis in filter-grown Madin-Darby canine kidney cells. *J. Cell Biol.* *109*, 3243–3258.
- Breitfeld, P., Casanova, J.E., Harris, J.M., Simister, N.E., and Mostov, K.E. (1989a). Expression and analysis of the polymeric immunoglobulin receptor. *Methods Cell Biol.* *32*, 329–337.
- Breitfeld, P.P., Harris, J.M., and Mostov, K.M. (1989b). Postendocytotic sorting of the ligand for the polymeric immunoglobulin receptor in Madin-Darby canine kidney cells. *J. Cell Biol.* *109*, 475–486.
- Breitfeld, P.P., McKinnon, W.C., and Mostov, K.E. (1990). Effect of nocodazole on vesicular traffic to the apical and basolateral surfaces of polarized MDCK cells. *J. Cell Biol.* *111*, 2365–2373.
- Brown, P.S., Wang, E., Aroeti, B., Chapin, S.J., Mostov, K.E., and Dunn, K.W. (2000). Definition of distinct compartments in polarized Madin-Darby canine kidney (MDCK) cells for membrane-volume sorting, polarized sorting and apical recycling. *Traffic* *1*:124–140.
- Brown, W.J., and Farquhar, M.G. (1989). Immunoperoxidase methods for the localization of antigens in cultured cells and tissue sections by electron microscopy. *Methods Cell Biol.* *31*, 553–569.
- Bucci, C., Wandinger-Ness, A., Lutcke, A., Chiariello, M., Bruni, C.B., and Zerial, M. (1994). Rab5a is a common component of the apical and basolateral endocytic machinery in polarized epithelial cells. *Proc. Natl. Acad. Sci. USA* *91*, 5061–5065.
- Cardone, M.H., Smith, B.L., Song, W., Mochley-Rosen, D., and Mostov, K.E. (1994). Phorbol myristate acetate-mediated stimulation of transcytosis and apical recycling in MDCK cells. *J. Cell Biol.* *124*, 717–727.
- Casanova, J.E., Wang, X., Kumar, R., Bhartur, S.G., Navarre, J., Woodrum, J.E., Altschuler, Y.A., Ray, G.S., and Godenring, J.R. (1999). Association of Rab25 and Rab11a with the apical recycling system of polarized Madin-Darby canine kidney cells. *Mol. Biol. Cell* *10*, 47–61.
- Chen, W., Feng, Y., Chen, D., and Wandinger-Ness, A. (1998). Rab11 is required for *trans*-Golgi network-to-plasma membrane transport and a preferential target for GDP dissociation inhibitor. *Mol. Biol. Cell* *9*, 3241–3257.
- Dunn, K.W., McGraw, T.E., and Maxfield, F.R. (1989). Iterative fractionation of recycling receptors from lysosomally destined ligands in an early sorting endosome. *J. Cell Biol.* *109*, 3303–3314.
- Fölsch, H., Ohno, H., Bonifacino, J.S., and Mellman, I. (1999). A novel clathrin adaptor complex mediates basolateral targeting in polarized epithelial cells. *Cell* *99*, 189–198.
- Fuller, S.D., and Simons, K. (1986). Transferrin receptor polarity and recycling accuracy in “tight” and “leaky” strains of Madin-Darby canine kidney cells. *J. Cell Biol.* *103*, 1767–1779.
- Futter, C.E., Gibson, A., Allchin, E.H., Maxwell, S., Ruddock, L.J., Odorizzi, G., Domingo, D., Trowbridge, I.S., and Hopkins, C.R. (1998). In polarized MDCK cells basolateral vesicles arise from clathrin-gamma-adaptin-coated domains on endosomal tubules. *J. Cell Biol.* *141*, 611–623.
- Gibson, A., Futter, C.E., Maxwell, S., Allchin, E.H., Shipman, M., Kraehenbuhl, J.P., Domingo, D., Odorizzi, G., Trowbridge, I.S., and Hopkins, C.R. (1998). Sorting mechanisms regulating membrane protein traffic in the apical transcytotic pathway of polarized MDCK cells. *J. Cell Biol.* *143*, 81–94.
- Goldenring, J.R., Soroka, C.J., Shen, K.R., Tang, L.H., Rodriguez, W., Vaughan, H.D., Stoch, S.A., and Modlin, I.M. (1994). Enrichment of rab11, a small GTP-binding protein, in gastric parietal cells. *Am. J. Physiol.* *267*, G187–G194.
- Gorvel, J., Chavrier, P., Zerial, M., and Gruenberg, J. (1991). rab5 controls early endosome fusion in vitro. *Cell* *64*, 915–925.
- Green, E.G., Ramm, E., Riley, N.M., Spiro, D.J., Goldenring, J.R., and Wessling-Resnick, M. (1997). Rab11 is associated with transferrin-containing recycling compartments in K562 cells. *Biochem. Biophys. Res. Commun.* *239*, 612–616.
- Gruenberg, J., Griffiths, G., and Howell, K. (1989). Characterization of the early endosome and putative endocytic carrier vesicles in vivo and with an assay of vesicle fusion in vitro. *J. Cell Biol.* *108*, 1301–1316.
- Hemery, L., Durand-Schneider, A.-M., Feldmann, G., Vaerman, J.-P., and Maurice, M. (1996). The transcytotic pathway of an apical plasma membrane protein (B10) in hepatocytes is similar to that of IgA and occurs via a tubular pericentriolar compartment. *J. Cell Sci.* *109*, 1215–1227.

- Hughson, E.J., and Hopkins, C. (1990). Endocytic pathways in polarized caco-2 cells: identification of an endosomal compartment accessible from both apical and basolateral surfaces. *J. Cell Biol.* *110*, 337–348.
- Hunziker, W., Mâle, P., and Mellman, I. (1990). Differential microtubule requirements for transcytosis in MDCK cells. *EMBO J.* *9*, 3515–3525.
- Hunziker, W., and Peters, P.J. (1998). Rab17 localizes to recycling endosomes and regulates receptor-mediated transcytosis in epithelial cells. *J. Biol. Chem.* *273*, 15734–15741.
- Ihrke, G., Martin, V.M., Shanks, M.R., Schrader, M., Schroer, T.A., and Hubbard, A.L. (1998). Apical plasma membrane proteins and endolyn-78 travel through a subapical compartment in polarized WIF-B hepatocytes. *J. Cell Biol.* *141*, 115–133.
- Knight, A., Hughson, E., Hopkins, C., and Cutler, D. (1995). Membrane protein trafficking through the common apical endosome compartment of polarized Caco-2 cells. *Mol. Biol. Cell* *6*, 597–610.
- McGraw, T.E., Dunn, K.W., and Maxfield, F.R. (1993). Isolation of a temperature-sensitive variant Chinese hamster ovary cell line with a morphologically altered endocytic recycling compartment. *J. Cell Physiol.* *155*, 579–594.
- Mostov, K., ter Beest, M.B.A., and Chapin, S.J. (1999). Catch the Symbol" § 121B. train to the basolateral surface. *Cell* *99*, 121–122.
- Mostov, K.E., and Cardone, M.H. (1995). Regulation of protein traffic in polarized epithelial cells. *BioEssays* *17*, 129–138.
- Mukherjee, S., Ghosh, R.N., and Maxfield, F.R. (1997). Endocytosis. *Physiol. Rev.* *77*, 759–803.
- Odorizzi, G., Pearse, A., Domingo, D., Trowbridge, I.S., and Hopkins, C.R. (1996). Apical and basolateral endosomes of MDCK cells are interconnected and contain a polarized sorting mechanism. *J. Cell Biol.* *135*, 139–152.
- Parton, R.G., Prydz, K., Bomsel, M., Simons, K., and Griffiths, G. (1989). Meeting of the apical and basolateral endocytic pathways of the Madin-Darby canine kidney cell in late endosomes. *J. Cell Biol.* *109*, 3259–3272.
- Ren, M., Xu, G., Zeng, J., De Lemos-Chiarandini, C., Adesnik, M., and Sabatini, D.D. (1998). Hydrolysis of GTP on Rab11 is required for direct delivery of transferrin from the pericentriolar recycling compartment to the cell surface but not from sorting endosomes. *Proc. Natl. Acad. Sci. USA* *95*, 6187–6192.
- Sheff, D.R., Daro, E.A., Hull, M., and Mellman, I. (1999). The receptor recycling pathway contains two distinct populations of early endosomes with different sorting functions. *J. Cell Biol.* *145*, 123–139.
- Simonsen, A., Lippé, R., Christoforidis, S., Gaullier, J.-M., Brech, A., Callaghan, J., Toh, B.-H., Murphy, C., Zerial, M., and Stenmark, H. (1998). EEA1 links PI(3) function to Rab5 regulation of endosome fusion. *Nature* *394*, 494–498.
- Song, W., Apodaca, G., and Mostov, K. (1994). Transcytosis of the polymeric immunoglobulin receptor is regulated in multiple intracellular compartments. *J. Biol. Chem.* *269*, 29474–29480.
- Stenmark, H., Aasland, R., Toh, B.-H., and D'Arrigo, A. (1996). Endosomal localization of the autoantigen EEA1 is mediated by a zinc-binding FYVE finger. *J. Biol. Chem.* *271*, 24048–24054.
- Ullrich, O., Reinsch, S., Urbe, S., Zerial, M., and Parton, R.G. (1996). Rab11 regulates recycling through the pericentriolar recycling endosome. *J. Cell Biol.* *135*, 913–924.
- van IJzendoorn, S.C.D., and Hoekstra, D. (1998). (Glyco)sphingolipids are sorted in sub-apical compartments in HepG2 cells: a role for non-Golgi-related intracellular sites in the polarized distribution of (glyco)sphingolipids. *J. Cell Biol.* *142*, 683–696.
- van IJzendoorn, S.C.D., and Hoekstra, D. (1999). The subapical compartment: a novel sorting center? *Trends Cell Biol.* *9*, 144–149.
- van IJzendoorn, S.C.D., Zegers, M.M.P., Kok, J.W., and Hoekstra, D. (1997). Segregation of glucosylceramide and sphingomyelin occurs in the apical to basolateral transcytotic route in HepG2 cells. *J. Cell Biol.* *137*, 347–357.
- Zacchi, P., Stenmark, H., Parton, R.G., Orioli, D., Lim, F., Giner, A., Mellman, I., Zerial, M., and Murphy, C. (1998). Rab17 regulates membrane trafficking through apical recycling endosomes in polarized epithelial cells. *J. Cell Biol.* *140*, 1039–1053.